Microfluidic Chemical Analysis Systems

Eric Livak-Dahl,[1,*] Irene Sinn,[2,*] and Mark Burns[1,2]

[1]Department of Chemical Engineering and [2]Department of Biomedical Engineering, University of Michigan, Ann Arbor, Michigan 48109; email: elivak@umich.edu, isinn@umich.edu, maburns@umich.edu

Annu. Rev. Chem. Biomol. Eng. 2011. 2:325–53

First published online as a Review in Advance on March 15, 2011

The *Annual Review of Chemical and Biomolecular Engineering* is online at chembioeng.annualreviews.org

This article's doi:
10.1146/annurev-chembioeng-061010-114215

1947-5438/11/0715-0325$20.00

*These authors contributed equally to this work and are listed alphabetically.

Keywords

assays, biochemical, microfabrication, droplet, laminar flow, microarrays

Abstract

The field of microfluidics has exploded in the past decade, particularly in the area of chemical and biochemical analysis systems. Borrowing technology from the solid-state electronics industry and the production of microprocessor chips, researchers working with glass, silicon, and polymer substrates have fabricated macroscale laboratory components in miniaturized formats. These devices pump nanoliter volumes of liquid through micrometer-scale channels and perform complex chemical reactions and separations. The detection of reaction products is typically done fluorescently with off-chip optical components, and the analysis time from start to finish can be significantly shorter than that of conventional techniques. In this review we describe these microfluidic analysis systems, from the original continuous flow systems relying on electroosmotic pumping for liquid motion to the large diversity of microarray chips currently in use to the newer droplet-based devices and segmented flow systems. Although not currently widespread, microfluidic systems have the potential to become ubiquitous.

INTRODUCTION

What is Microfluidics?

Microfluidics is the science and engineering of systems that manipulate small amounts of fluids at length scales from a few micrometers up to a millimeter (1). The design and use of microfluidic devices for fluid transport have found many applications in the life sciences, particularly in biochemical analysis and the pharmaceutical industry, and in other areas including chemical syntheses and environmental testing. Passively or actively controlled microfluidic components, such as mixers, actuators, reactors, separators, sensors, valves, and pumps, have been developed for transport processes and fluid control (2). The strength of microfluidic systems lies in their integration ability (**Figure 1**); this has led to the rapid expansion of the field and development toward micrototal analysis systems (μTASs), commonly known as lab-on-a-chip systems (3). These idealized integrated devices incorporate sample preparation, handling, detection, and analysis (4), and they enable high-throughput screening studies and strive for simple incorporation in a user-friendly, automated system (5). Furthermore, their parallel analysis capabilities, short reaction and/or separation times, and reduced reagent volumes allow microfluidic technologies to revolutionize biological and chemical assays (6).

Concepts at the Microscale for Fluid Flow

The physical properties of microsystems are governed by scaling laws that express the variation of physical quantities with the length scale, l, of a given system or object, provided that other external quantities such as time (t), pressure (p), and temperature (T) remain constant (7). For instance, a general scaling law frequently used for microfluidic systems expresses the ratio of surface forces, such as surface tension and viscosity, to volume forces, such as gravity and inertia, as a system's dimensions are reduced. This scaling law can be expressed as

$$\frac{\text{surface forces}}{\text{volume forces}} \propto \frac{l^2}{l^3} \propto l^{-1} \xrightarrow[l \to 0]{} \infty, \qquad 1.$$

Figure 1

Integrative, high-throughput, parallel-processing microfluidic systems for chemical assay applications that incorporate continuous flow systems, microarray systems, and droplet systems. (*a*) A disc-based, automated enzyme-linked immunosorbent assay (ELISA) system using innovative laser irradiated ferrowax microvalves (LIFM) to test for infectious diseases from whole blood within 30 min. The numbers indicate the order of the LIFM operation. TMB is tetramethyl benzidine, a visualizing agent. Figure reproduced with permission from Reference 13, copyright © 2009, The Royal Society of Chemistry. (*b*) A multilayer microfluidic immunoassay system containing microvalves and micropumps for the rapid and high-throughput detection of chemical compounds. The system is composed of three layers, the upper fluidic and lower pneumatic control layers, which are separated by a thin polydimethylsiloxane (PDMS) membrane. Roman numerals I–V represent the valve control lines for the parallel system, and numbers 1–5 represent fluidic control valves for one system. Reproduced with permission from Reference 14, copyright © 2009, The Royal Society of Chemistry. (*c*) An integrated blood barcode chip (IBBC) using DNA-encoded antibody library (DEAL) barcode arrays. The system rapidly and selectively samples a large panel of protein markers from whole blood (red blood cells, white blood cells, and plasma proteins). A–C represent DNA codes, and numbers 1–5 represent DNA-antibody conjugate, plasma protein, biotin-labeled detection antibody, streptavidin-Cy5 fluorescence probe, and complementary DNA-Cy3 reference probe, respectively. Reprinted with permission from Macmillan Publishers Ltd.: *Nature Biotechnology*, Reference 15, copyright © 2008. (*d*) A high-density DNA microarray system for genetic and gene expression analysis at the whole-genome level by monitoring hybridization to open reading frames (ORFs) (16). Copyright © 1997 National Academy of Sciences, U.S.A. (*e*) A schematic of a droplet microfluidic system for genetic analysis that uses restriction endonuclease digestion (RD) and polymerase chain reaction (PCR) amplification followed by electrophoresis. V, valve; L, liquid entry channel; B, buffer channel; E, applied electric field; A, air output. Reproduced with permission from Reference 11, copyright © 2005, The Royal Society of Chemistry.

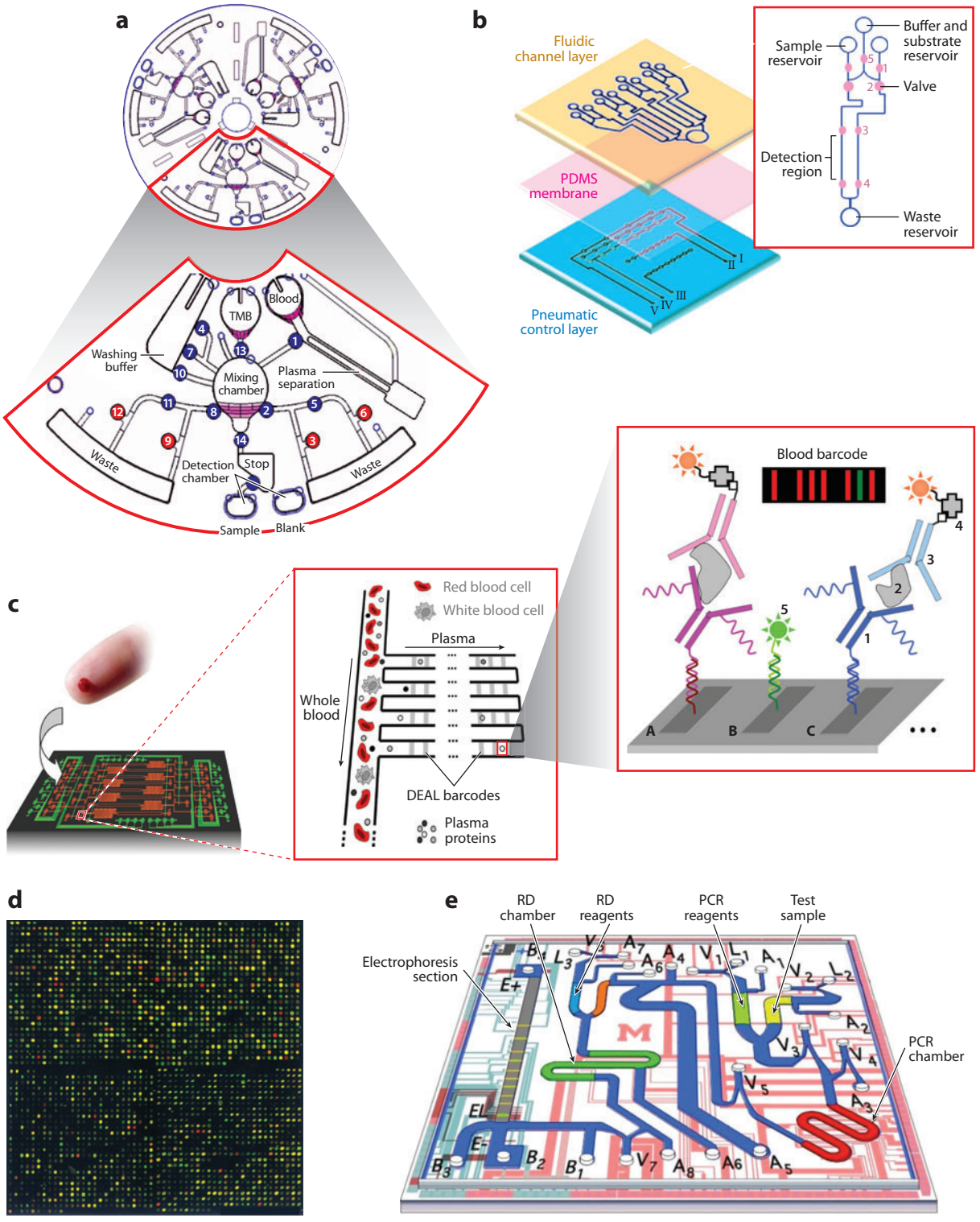

Table 1 Change in physical quantities with miniaturization

Physical quantity	Change		Length scale
Linear flow rate	Reduced	On the order of	l^1
Volumetric flow rate	Reduced		l^3
Diffusive rate	Increased		l^2
Driving pressure	Increased		l^4
Gravity effects	Reduced		l^3

where l is the length scale and indicates the importance of surface forces in these micrometer-based systems (2). Important scaling laws as a function of l for several physical quantities are presented in **Table 1**.

In addition to scaling laws, dimensionless numbers, as shown in **Table 2**, provide further insight into the physical phenomena occurring in microfluidic devices. Such numbers are derived from fundamental equations governing the behavior of fluid flow (8). For instance, the simplified Navier-Stokes equation is

$$\rho \frac{d\mathbf{u}}{dt} = -\nabla p + \eta \nabla^2 \mathbf{u} + \mathbf{f}, \qquad 2.$$

Table 2 Change in dimensionless groups with miniaturization

Dimensionless name and symbol	Quantity	Definition	Change		Length scale
Reynolds (Re)	$\frac{\rho U_0 L_0}{\eta}$	$\frac{\text{Inertial forces}}{\text{Viscous forces}}$	Reduced	On the order of	l^2
Péclet (Pe)	$\frac{U_0 L_0}{D}$	$\frac{\text{Fluid convection}}{\text{Fluid diffusion}}$	Reduced		l^2
Capillary (Ca)	$\frac{\eta U_0}{\gamma}$	$\frac{\text{Viscous forces}}{\text{Interfacial forces}}$	Reduced		l^1
Damköhler (Da)	$\frac{D\tau_R}{L^2}$	$\frac{\text{Reaction time}}{\text{Transport time}}$	Increased		l^0
Marangoni (Mg)	$\frac{\Delta\gamma R}{\eta\alpha}$	$\frac{\text{Surface tension gradient}}{\text{Viscous forces}}$	Reduced		l^1
Bond (Bo)	$\frac{\Delta\rho g R^2}{\gamma_i}$	$\frac{\text{Gravity}}{\text{Surface tension}}$	Reduced		l^2
Sherwood (Sh)	$\frac{\kappa L}{D}$	$\frac{\text{Convective mass transport}}{\text{Diffusive mass transport}}$	Reduced		l^1
Deborah (De)	$\tau\left(\frac{\gamma}{\rho R^3}\right)^{1/2}$	$\frac{\text{Relaxation time for polymeric liquid}}{\text{Characteristic time}}$	Increased		$l^{3/2}$
Knudsen (Kn)	$\frac{\lambda}{L}$	$\frac{\text{Mean free path}}{\text{Physical length scale}}$	Increased		l^1
Weber (We)	$\frac{\rho V^2}{\gamma/R}$	$\frac{\text{Inertial forces}}{\text{Surface tension forces}}$	Reduced		l^3

where ρ is the fluid density, **u** is the fluid velocity vector, η is the viscosity, and **f** represents body forces (8). The most commonly used dimensionless parameter in microfluidic systems obtained by making the above equation dimensionless is the Reynolds number,

$$Re = \frac{\rho U_0 L_0}{\eta}, \qquad 3.$$

where U_0 is the characteristic velocity and L_0 is the characteristic length. The Reynolds number compares the relative importance of inertial effects and viscous effects; at the dimensions employed by microfluidic devices, the Reynolds number is sufficiently low (typically $Re \ll 2{,}000$) that viscous forces dominate, resulting in laminar flow conditions (8, 9). The Péclet number, another important dimensionless parameter obtained from the same equations, compares the convective and diffusive or dispersive effects in channels. This number indicates the degree and form of mixing in fluid samples and is important when designing devices for sensing and separating flow sources and ingredients (8). At the dimensions used in microfluidic devices, the Péclet number is sufficiently small that diffusion dominates fluid mixing. The Reynolds and Péclet numbers, in addition to other dimensionless numbers, are listed in **Table 2**; these parameters provide insight to the microscopic flow properties in unique microfluidic systems and are explained in detail within subsequent sections.

Why Microfluidic Chemical Assays?

Microfluidic continuous flow, microarray, and droplet-based systems have increasingly been used in the miniaturization of large-scale chemical assays and analytical techniques (**Figure 1**). Microfluidics enables a high degree of fluid control while simultaneously using a near-trivial amount of expensive reagents. The incorporation of liquid handling, temperature control, and target detection components into a single device allows for analysis and screening procedures to be completed at greater speeds, with higher throughput and yield, and with improved selectivity compared to their lab-scale counterparts (10). For instance, downscaling DNA analysis methods results in extremely efficient devices—the thermal cycling necessary for PCR (polymerase chain reaction, i.e., DNA amplification) can rapidly be performed because of the incorporation of temperature controllers, the efficient heat transfer, and the tiny thermal mass (10, 11). In addition, the ability to densely pack microfluidic channels and components together on a device (12) that is essentially photocopied allows for the economical production of highly parallelized systems for high-throughput analytical studies (13–16). Significant technological advances have been made in the burgeoning field of microfluidics; however, many of the systems remain in the proof-of-concept stage (1). As a result, the full potential of microfluidics will remain unknown until the transition to widespread commercialization occurs. In this article, we review a variety of concepts that contribute to the construction of highly integrated microfluidic systems and how these concepts have been applied in chemical analysis applications.

CONTINUOUS FLOW ASSAYS

Principles of Flow Control

The first microfluidic chips used continuous streams of liquid in the channels, and the first widespread technique for controlling this flow was electroosmosis. Electroosmotic control was first developed for flow control in capillary electrophoresis (CE). Also known as capillary zone electrophoresis (CZE), CE first arose in the early-to-mid-1980s as a separation technique

complementary to gel-based electrophoresis and high-performance liquid chromatography (HPLC), and was used for separating electrolytes in solution (17, 18). In addition to the electrophoretic motion separating the solutes, electroosmotic flow also moves the bulk liquid.

The phenomenon of electroosmosis arises from the electrolytes in solution equilibrating with the surrounding channel walls, forming an ionic double layer—the Debye layer—near the solid-liquid interface. An applied electric field then causes this layer to migrate, resulting in bulk flow throughout the capillary. This flow can be modeled simply by including an extra term for electrical forcing in the Navier-Stokes equation,

$$\rho \frac{d\mathbf{u}}{dt} = -\nabla p + \eta \nabla^2 \mathbf{u} + \rho_e \mathbf{E}_{\mathbf{ext}}, \quad 4.$$

where ρ is the fluid density, $\mathbf{u}$ is the flow velocity vector, p is the pressure, η is the dynamic viscosity of the fluid, ρ_E is the electric charge density in the double layer, and E_{ext} is the external applied electric field (19).

By the mid-1990s, the technique had been developed into a general tool for fluid pumping and controlling microfluidic environments distinct from CE applications (20). Through the continuous application and manipulation of voltages, the technique, originally developed in glass capillaries, can be successfully applied in polydimethylsiloxane (PDMS), silicon, or glass microchannels (21). In addition to ease of control, the other major attraction of electroosmotic flow is that the fluid velocity is not hindered by decreasing the channel dimensions.

Pressure-driven flow, however, is severely affected by the channel dimensions but is the most straightforward microfluidic flow control technique. Analogous to macroscale fluid pumping, microfluidic pressure-driven flow can be used in either a constant pressure or a constant displacement mode. Early use focused on both gas and liquid flow (22), but today liquid is the predominant fluid medium. Flow that is laminar, incompressible, and viscous, in a pipe with its length much greater than its diameter—criteria met by microfluidic flow—is described by the Hagen-Poiseuille equation,

$$\Delta P = \frac{12 \eta L Q}{\pi d^4}, \quad 5.$$

where ΔP is the pressure drop across length L of pipe with diameter d, for a flow rate Q of a fluid with viscosity η. As the channel diameter decreases, the pressure needed to achieve the same flow rate increases dramatically.

The simplest techniques for pressure-driven flow use macroscale pressure sources, such as a pressurized fluid reservoir or a vacuum source, connected to the microfluidic device, rather than microscale sources located on-chip. Alternatively, constant volumetric flow can be used (e.g., a syringe pump), but care must be taken to avoid high pressures in the connecting tubing. Both cases necessitate bulky external equipment; for some applications this is acceptable. For portability and/or small size, various designs for on-chip micropumps have been developed (23). Many of these designs are based on flow driven by a diaphragm—piezoelectric driving is common—but others rely on magnetic driving or acoustic streaming (24).

Another technique prominent at the microscale is the use of surface forces to control flow. Because of the increased surface area-to-volume ratio, interfacial interactions between the fluid and the channel walls can be used to pump fluids through the device (25). Alternatively, capillary pressure-driven flows can be generated by using heat to alter the surface tension (26). Like pressure flow, capillary flow can be described by the Hagen-Poiseuille equation with the addition of a capillary pressure term (27):

$$\Delta P = P_{\text{capillary}}, \quad 6.$$

$$P_{\text{capillary}} = \frac{2\gamma \cos\theta}{r}, \quad 7.$$

where γ is the surface tension, θ is the contact angle between the fluid and the channel wall, and r is the radius of the channel.

Similar to electroosmotic flow, gravity-driven or hydrostatic flow was first studied in the microfluidic regime in relation to CE. Initially viewed as problematic, as it contributed to zone broadening in CE (28), it was later developed into a flow control technique of its own. Gravity-driven flow is generated either through tilting the entire device (29) or by filling an inlet reservoir to a height greater than that of the device channels; the former obviates the need for external equipment such as an adjustable stage, whereas the latter allows precise control of a constant volume rate. And similar to electroosmotic flow, gravity-driven flow can be described by the addition of a term to the Navier-Stokes equation,

$$\rho \frac{d\mathbf{u}}{dt} = -\nabla p + \eta \nabla^2 \mathbf{u} - \rho \mathbf{g}^* z, \quad 8.$$

where $g* = g + \omega r^2$ and combines both gravitational and centrifugal forces. In addition to portability and lack of external power or pressure requirements, gravity-driven flow offers the advantage of gentleness, an important consideration in applications such as flow cytometry of cells (30). A related technique is the use of centrifugation to drive sample flow in compact disc (CD)-sized lab-on-a-disc devices (31). Samples and reagents are loaded onto the disc, which is usually made of poly(methyl methacrylate) (PMMA) in the size and shape of a CD or digital video disc (DVD). The disc is then spun in a standard disc drive to carry out the analysis operations. This technique has the advantage of using commonplace consumer-level equipment to operate, and some devices are even being designed to use the laser in DVD drives for various tasks.

Phenomena and Components for Chip-Based Assays

Many phenomena and components can be used to build microfluidic array systems. One of the most exploited phenomena on the microscale is the laminar nature of microscale flows. This eddy-free flow allows for the formation of segregated composition in regions generated by combining distinct chemical streams. At high Péclet numbers—readily achievable at the microscale—these boundaries can be easily maintained (32). The dimensions and duration of the gradient streams depend on the Péclet number and can be approximated with the relation:

$$D = L^2/t. \quad 9.$$

The investigation of many biological or chemical phenomena, such as cell signaling and chemotaxis, involves concentration gradients (33). By using branched networks of channels with appropriate hydrodynamic resistances, an inlet stream can be repeatedly diluted and mixed to create gradients with different concentration profiles (34). Simple networks produce linear profiles, whereas complex networks can generate double peaks, sawtooth patterns, and other more complicated shapes (35, 36). The gradients can also be used to create complex topography in microfluidic channels by generating gradients in chemical etchant concentrations.

Although the laminar nature of microfluidic flow allows the generation of sharp gradients, this lack of turbulent flow can hinder mixing of reagents. At smaller length scales (i.e., submicrometer), diffusive mixing occurs on the order of milliseconds. However, in microfabricated structures, which may be hundreds to thousands of micrometers wide, complete mixing in stagnant fluid may take as long as an hour, and innovative strategies have been developed to overcome this delay. For

instance, oscillating electroosmotic flow can induce an electrokinetic instability that results in rapid mixing (37). In other flow modes, mixing can be induced by clever channel design (38) or by patterning wells, hydrophobic patches (39), or other disruptions on the floor of the channel, resulting in a high degree of mixing within a few hundred micrometers (40). In droplet systems, simply moving the drop causes recirculation of the liquid and, for the correct velocity and travel time, mixing can occur in fractions of a second. Solute adsorption to the channel surface must be considered and can be minimized by surface coating strategies such as radio-frequency glow discharge plasma deposition (RF-GDPD) or by preparing the surface with a known adsorbed protein (41).

Valves are one of the most basic components of microfluidic arrays and have been constructed using both hard (e.g., silicon and glass) and soft (e.g., PDMS) substrates (**Figure 2**). By far the most common is the multilayer elastomeric PDMS valve that applies pressure or vacuum to one channel in order to squeeze closed or expand open adjacent channels (42, 43). Through clever design, multiplexers using binary valve patterns in a combinatorial array can operate hundreds or thousands of these individually addressable valves to produce chips that can perform massively parallel operations (12). Plug-type valves are the most common active valves made from hard substrates. These include both valves that polymerize in place (44) and those that are wax-like. Wax valves have the added advantage that they can be electronically addressed by melting with on-chip electrical heaters, thus limiting the required external connections (45).

Formation of complete assay systems relies on combining valves and phenomena into a complete working system. Most often, this requires constructing a reaction chamber (i.e., merely a section of channel), performing a reaction, and then detecting the extent of that reaction. The most prevalent example of this is the detection of specific DNA sequences using PCR. Glass capillaries had been used to reduce sample volumes and speed the requisite heating and cooling cycles for PCR, but fluid handling remained a challenge until the technique was integrated into microfabricated devices (46). Generally, heating is accomplished on-chip using polysilicon or metal for electrical heating. Packed bead reactor chambers have also been developed with both magnetic and nonmagnetic beads (47).

Detection of completed PCR reactions is predominantly conducted by adding fluorescent dyes and electrophoretically separating DNA strands. As we have discussed, the first microfluidic devices used electric fields to pump fluids; these fields can also be used to separate ionic species (e.g., DNA) with the addition of linear polymers to achieve the desired resolution. Gel matrices can be incorporated into microfluidic devices to attain an even higher resolution for the same length channel, and these gel systems have been used for DNA/RNA or protein separations on-chip with the same techniques used at the macroscale. Use of liquid chromatography has been more limited owing to the difficulties involved in high-pressure applications at the microscale, but some work has been conducted (48). Recently, use of surface plasmon resonance (SPR) imaging techniques in microfluidic devices has been increasing; SPR is attractive because it requires no labeling (49). In addition to separation, concentration of species is also possible, usually through the use of nanochannels to generate exclusion regions or extended space charge regions (50). Concentrations of proteins or other analytes on the order of a million-fold have been reported.

Processing of the reaction products typically is not done in microfluidic systems although devices for postreaction processing have been developed including sample fraction collection, labeling, and sorting (51). Postreaction processing is widely used in sorting systems, particularly in cell flow cytometry. The small sample volumes and precise fluid control make microfluidic devices well-suited for this application. Furthermore, the transparency of glass and PDMS substrates allows cells or particles to be detected and sorted fluorescently (52). Other sorting schemes take advantage of the laminar nature of microfluidic flow. By flowing a particle solution through an

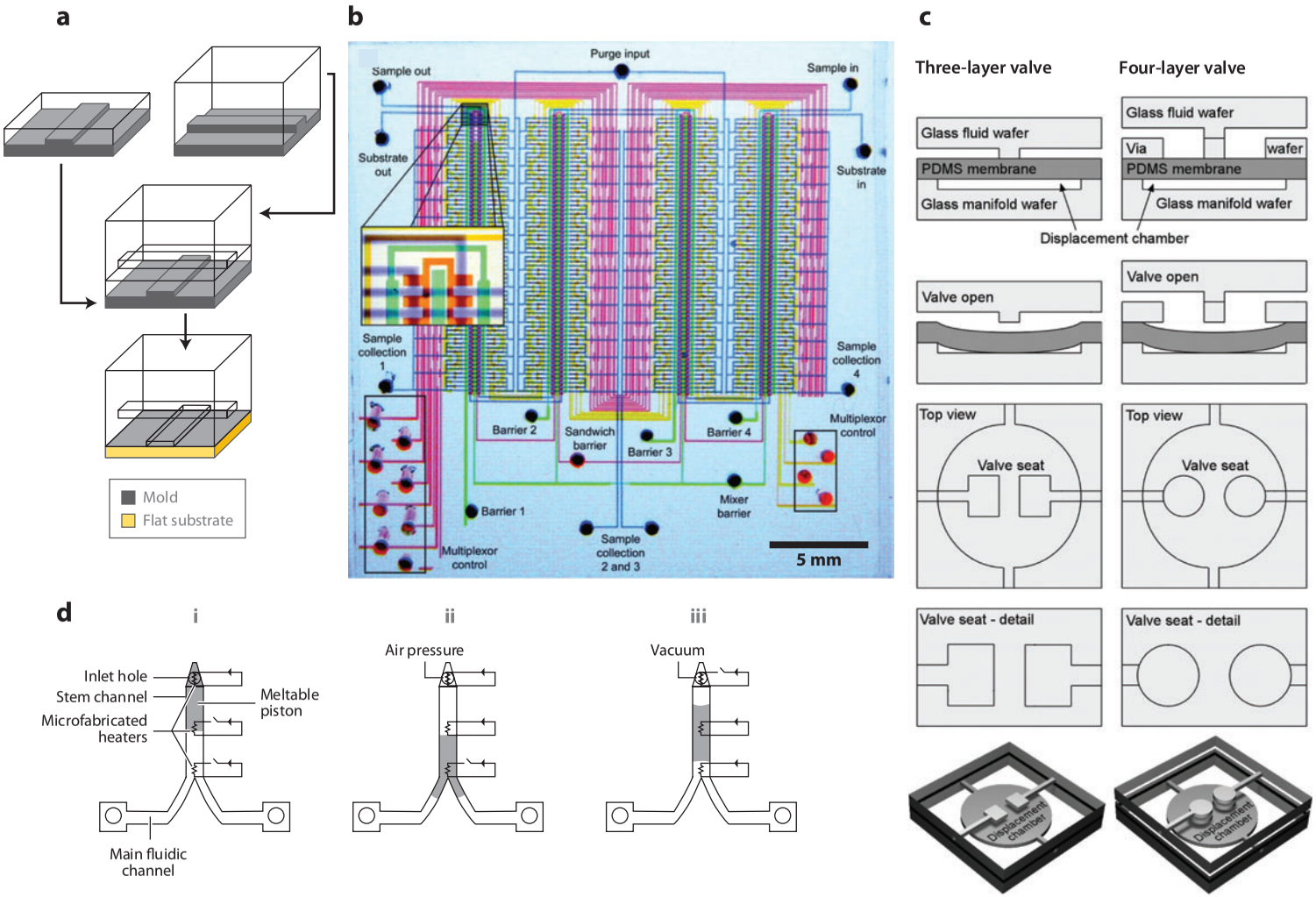

Figure 2

A variety of microfluidic valve designs. (*a*) Multilayer polydimethylsiloxane (PDMS) channels allow pressure in one channel to pinch off flow in an adjacent channel. From Reference 42; reprinted with permission from AAAS. (*b*) PDMS valves, as shown in (*a*), are multiplexable on large scales. From Reference 12; reprinted with permission from AAAS. (*c*) PDMS membranes can be used to construct valves in glass devices as well, thus combining the ease of elastomer-based valves with the advantages of glass surface chemistry. Reproduced with permission from Reference 43, copyright © 2003, Elsevier. (*d*) Alternative approaches include phase transition-based valves such as this one involving melting wax. Reproduced with permission from Reference 45, copyright © 2004, American Chemical Society.

array of pillars of appropriate dimensions, smaller particles can be made to travel with the fluid while the pillars bump larger particles across streamlines (53). This technique can also be applied to cells (54) and their lysis products (55) to separate larger cell components such as chromosomes from smaller proteins and membrane fragments. Acoustic techniques such as acoustic differential extraction have also been developed and offer enhanced efficiency compared with macroscale techniques (56). Aside from physical methods, the aforementioned transparency of common device substrates makes them compatible with optical techniques as well. For example, by introducing a 3D optical lattice into the microfluidic device, particles can be sorted precisely and accurately on the basis of their size (57).

A natural application for microfluidic devices is the study of small-scale biological samples, especially cells (58, 59). Arrays of individually addressable microchambers allow cells to be exposed to a variety of extracellular conditions and monitored for changes in a multiplexed approach (60, 61). Particles with unique patterns to act as barcodes can be fabricated; these contain distinct analytical targets (62). Arrays of microposts can force cells into different shapes as they grow and have revealed strong effects of shape on cell behavior and differentiation (63).

HETEROGENEOUS ASSAYS: ARRAY CHIPS

The first microarray chips were based on principles similar to those of macroscale assays such as Southern blotting for DNA or tissue core blocks for tissue samples. As microtechnology evolved, the application of these principles expanded and resulted in increasingly powerful devices. For example, in 1987 the use of DNA spotted onto filter paper for gene expression analysis was first reported with an array of tens of samples (64). By 1995, microarray technology was able to produce a single array with 20,000 complementary DNA (cDNA) targets, and in 1997, the first complete eukaryotic genome-on-a-chip was reported for yeast (16). The initial tissue sample arrays consisted of approximately 100 samples in a paraffin block (65); less than ten years later, blocks could contain 1,000 samples, each of which could be subject to 200 different tests (66).

These techniques soon were applied to other applications (**Figure 3**). Proteins of various kinds (67), especially antibodies (68), have proven very useful for probing the proteomes of different organisms, starting with yeast in 2001 (69). In addition to gene analysis, gene synthesis can be carried out and multiplexed on array chips (70). MicroRNAs (miRNAs)—small noncoding RNAs that regulate gene expression—are thought to be involved in many diseases and are widely investigated; microarray technology has proven useful for monitoring miRNA expression levels as well (71). Finally, libraries of other chemical compounds can be arrayed and tested for interactions with biological or other samples (72). Current efforts to reduce the cost of genome sequencing for personalized medicine include the use of pyrosequencing on array chips, arrays of zero-mode waveguides for real-time sequencing analysis (73), and arrays of self-assembling DNA nanoballs (74).

Figure 3

Array chip technology advancement over time. (*a*) The earliest DNA arrays were fabricated through manual spotting on filter paper (64). (*b*) High-speed robotic printing allowed the creation of DNA microarrays. From Reference 92; reprinted with permission from AAAS. (*c*) Today, commercial DNA array chips can search for almost a million single-nucleotide polymorphisms (SNPs) across the whole human genome. Copyright © 2008, Affymetrix. (*d–f*) Array technology is versatile, allowing multiplexing analysis of proteins, RNA, and nonbiological chemicals as well as on-chip synthesis of genes. Panel *d* from Reference 70, reprinted by permission from Macmillan Publishers Ltd: *Nature*, copyright © 2004. Panel *e* from Reference 72, copyright © 2003, National Academy of Sciences, U.S.A.; Panel *f* from Reference 93, reprinted with permission from AAAS.

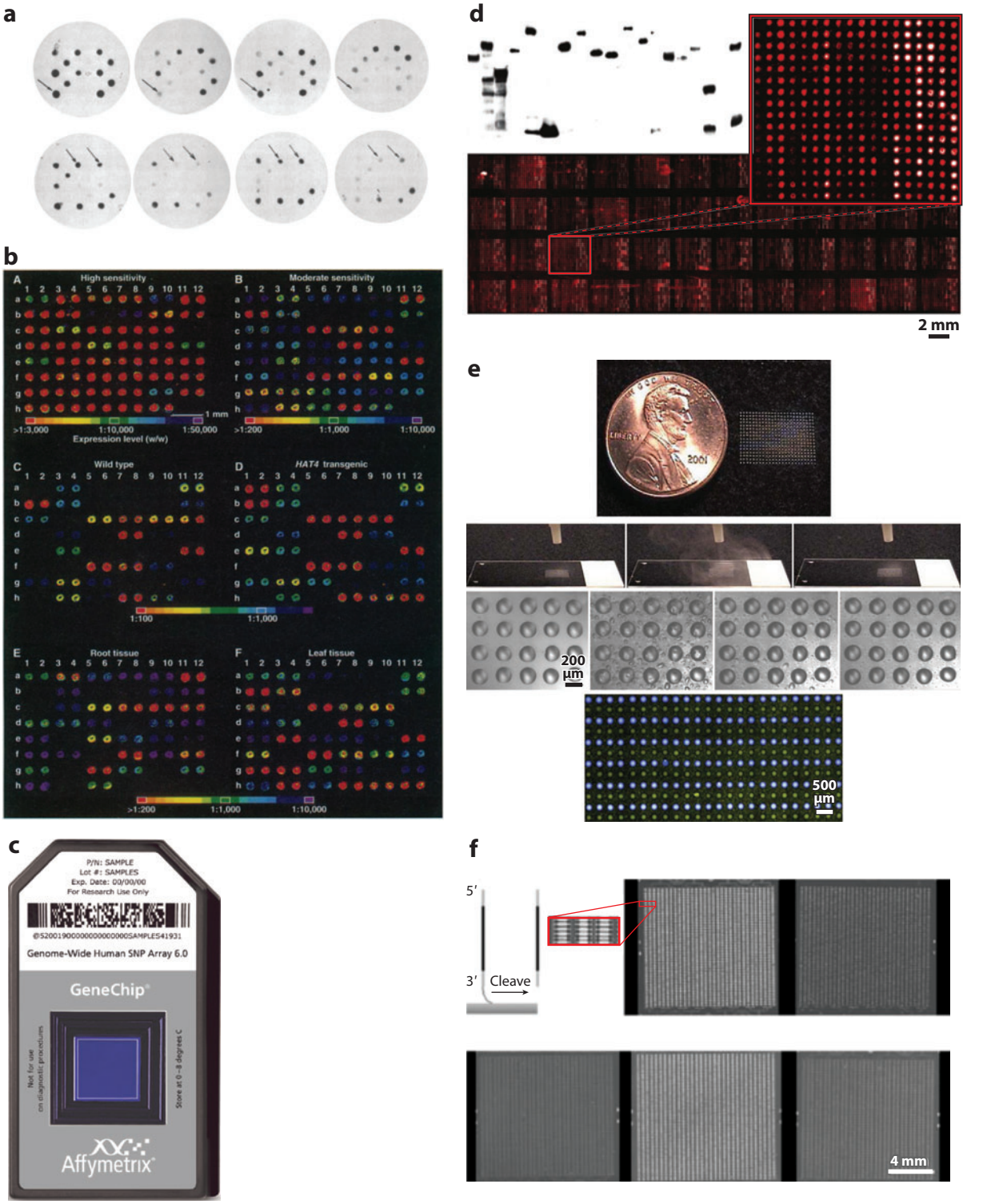

Array Fabrication

Microarray chips typically perform heterogeneous reactions (i.e., the reaction occurs at the surface rather than in the bulk), and thus their fabrication is more complicated than that of standard microfluidic systems. Photolithography is the standard procedure used to fabricate such chips because the patterning can access each location on the array containing a photolabile protecting group. Through use of a mask or other spatially addressable technique, light is used to selectively remove protecting groups (75). The desired building block molecule, which often is a specific nucleotide or amino acid, can be added sequentially to the deprotected locations and subsequently reprotect the selected area. As a result, different molecules can be synthesized in situ at different locations on the array; combinatorial strategies can be used to optimize the specific protocol (76). Such array chips are limited by the resolution of light (similar to the Rayleigh criterion for optical observation) unless more advanced fabrication techniques such as electron-beam patterning are used. For well-based arrays that perform homogeneous reactions, the loading of the individual reagents into each well, not the fabrication of the wells themselves, presents the bulk of the challenge.

Another widespread fabrication method is deposition, or spotting. Rather than synthesizing the molecules directly on the chip, molecules are synthesized separately and sequentially bound to the substrate. This technique has been useful for the creation of chips with arrays of long molecules whose individual photolithographic synthesis would be overly complicated (77). For example, DNA microarrays synthesized in situ are often on the order of tens of base pairs; spotted DNA microarrays are commonly on the order of hundreds of base pairs (78, 79). The two most common deposition methods are pin-based fluid transfer (80) and piezoelectric inkjet-based printing (81). After transfer of the fluid to the substrate, a reaction with the functionalized surface covalently bonds the molecules to the chip.

Reading and Analyzing Arrays

Subsequent to fabrication and hybridization of the reagents or samples, the array chip must be read spatially to determine the result of the assay. The most common methods involve hybridization of a probe followed by detection of that probe through fluorescence. This process is dictated by the interplay between mass transfer of the probes and the rate of the hybridization reaction (i.e., the Damkohler number). For example, hybridization of fluorescent probes is useful for detecting single nucleotide polymorphisms (SNPs) and other small changes in genetic sequence (76). Sandwich assays are a powerful tool for microarray protein detection applications. By combining protein sandwich assays with DNA array chip-based detection, attomolar detection of protein analytes has been reported (82).

Rather than hybridize probes to the sample, analysis can also be conducted by monitoring on-chip reactions with the sample as they occur. For example, one DNA sequencing method uses an array of DNA fragments in wells on an optical fiber chip (83). Pyrosequencing (84) is then carried out in each well, and the photon release associated with each nucleotide-incorporation event is detected. Thus, as the sample DNA fragment is replicated, it is also sequenced. Other methods rely on spatial detection of incorporation events; for example, binding sample DNA to a substrate, incorporating fluorescent nucleotides base by base, and observing this incorporation optically (85).

Analysis of the collected data from array chips can be performed by many techniques. One approach used in gene expression analysis is to cast a wide net with a chip containing random sequences of cDNA. Transcribed mRNA produced under a variety of physiological conditions can

then be bound to the chip, and, through fluorescent detection, the differences are noted. Regions containing differences across conditions can then be sequenced and analyzed (86). Gene expression can also be studied with cluster analysis (87), a standard statistical tool wherein individual data points are grouped algorithmically into clusters. These algorithms allow genes to be arranged according to similarity in function, which can provide insight into the purpose of unknown genes in light of their clustering with known genes. A wide selection of clustering algorithms is available including hierarchical, portioning, and density-based methods (88).

Additionally, significance analysis of microarrays (SAM) can be used to determine which alterations in gene expression are statistically significant with gene-specific *t* tests (89). The basic SAM algorithm consists of (*a*) ordering test statistics according to magnitude, (*b*) computing the ordered null (unaffected) scores for each permutation, (*c*) plotting the ordered test statistic against the expected null scores, (*d*) calling each gene significant if the absolute value of the test statistic for that gene minus the mean test statistic for that gene is greater than a stated threshold, and (*e*) estimating the false discovery rate based on expected versus observed values (90, 91). The need for biological statistical analysis that the widespread use of large-scale sequencing and array chip technology (92, 93) demands gave rise to the field of bioinformatics.

DROPLET MICROFLUIDICS

Droplet-based microfluidic systems enable the miniaturization and compartmentalization of reactions into picoliter- to microliter-volume droplets that are separated by a second immiscible fluid. Droplets remain mobile in closed-conduit and open-conduit microfluidic channels, similar to continuous flow systems; however, the droplets behave as isolated chambers that allow reactions to be performed in parallel without cross-contamination or sample dilution. Furthermore, reactions are not required to be stationary, as in array chips. As a result, microfluidic droplet-based systems provide a high-throughput platform for biological and chemical research.

One of the first droplet-based assay systems was the continuous gas-segmented flow analysis (SFA), also known as a continuous flow analysis (CFA), system. In the SFA-based AutoAnalyzer developed in the 1950s by Skeggs, an aqueous stream was segmented into liquid slugs separated by air bubbles (i.e., the second immiscible fluid) (94). This technological advance significantly increased the number and rate of sample processing events, as each slug acts as a distinct reaction microchamber. The isolation of each droplet prevented sample interaction, carryover, and dilution by reducing longitudinal dispersion effects (95, 96). Nevertheless, the compressibility of air resulted in uncontrolled fluid behavior; this issue is addressed with the use of water-in-oil droplets.

Isolation and Compartmentalization

Picoliter- to nanoliter-sized droplets in closed conduit systems are typically generated with passive methods by introducing nonlinearity and instability into laminar, two-phase microfluidic flow systems (97) (**Figure 4*a***). Two or more streams of immiscible fluids are combined at a rate large enough to allow shear force at the fluid interface to break one continuous phase into discrete droplets (98). The immiscibility of the two phases ensures the isolation and compartmentalization of each phase. The geometry of the junctions varies; however, the basic droplet formation method typically involves coflowing streams emerging from a common origin or cross-flowing streams entering a T-junction (99).

Droplet formation is governed by the capillary number, $Ca = \frac{\eta U_0}{\gamma}$, where η (Pa s) and U_0 (m s^{-1}) are the viscosity and velocity of the continuous phase, respectively, and γ (N m^{-1}) is the interfacial tension between the immiscible phases (100). At low capillary numbers

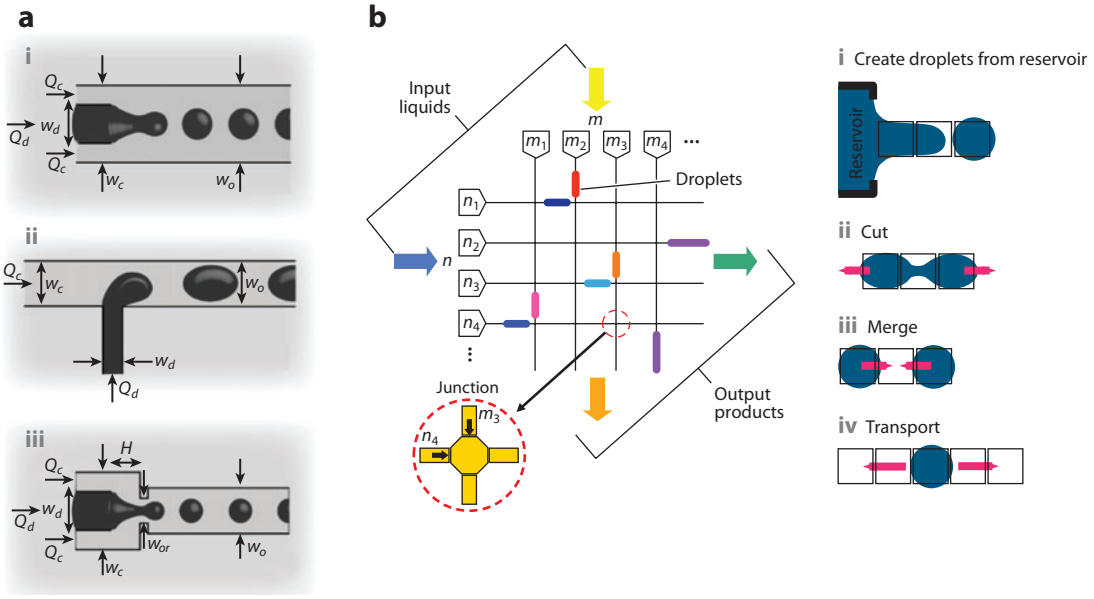

Figure 4

Droplet formation using passive and active mechanisms. (*a*) Passive droplet formation using coflowing streams (*top*), cross-flowing streams at a T-junction (*middle*), and flow focusing (*bottom*). Q_c, flow rate of continuous phase; Q_d, flow rate of disperse phase; w, width; H, height. Reproduced with permission from Reference 99, copyright © 2007, IOP Publishing. The size of the droplets can be controlled by adjusting the flow and liquid parameters. (*b*) In active droplet formation, the surface tension of the droplet can be adjusted by the application of a voltage, which causes the droplet to wet the substrate surface. By adjusting the strength and the number of sequential electrodes that are activated or deactivated, a droplet can be pinched off from the liquid reservoir; m and n represent the number of columns and rows, respectively, on the device. (*i*) A droplet can be formed if the electrode separating the liquid arm and a reservoir is deactivated, which causes the droplet to pinch off. Droplets can be (*ii*) split if opposite electrodes or (*iii*) merged if the adjacent electrode is activated. (*iv*) Droplets can also be transported by sequential activation of neighboring electrodes. Reproduced with permission from Reference 108, copyright © 2011, IEEE.

(i.e., $Ca < 10^{-2}$) the interfacial force dominates the shear stress, and the ratio of the volumetric flow rates between the two immiscible fluids governs droplet formation dynamics (101). When $Ca > 10^{-2}$, the shear stress dominates, and the channel dimensions, channel geometries, and fluid flow properties all influence the droplet breakup process (101). Passive droplet generation techniques are ideal for experimental conditions requiring a large number of droplets, such as high-throughput or parallel analysis applications (e.g., large-scale PCR) (102) or cell culturing techniques (103). Furthermore, the composition of the neighboring droplets can be controlled by adjusting the relative concentration of the upstream aqueous solution (104). This control is especially useful for chemical analysis applications such as enzymatic assays (104, 105), drug discovery assays (105), and protein crystallization techniques (104) in which various concentrations of initial analyte or solutions must be tested to optimize a procedure (104).

Droplets can also be formed with active mechanisms (**Figure 4*b***). Recently, surface acoustic wave (SAW) and electrohydrodynamic (EHD) techniques increasingly have been used; these processes are commonly performed in open conduits and do not require any external pumps. SAW relies on the creation of an acoustic pressure gradient in the droplet along the direction of wave propagation; the gradient creates a force in the same direction and induces fluid flow (106). Nevertheless, EHD methods such as dielectrophoresis (DEP) and electrowetting on dielectric (EWOD) remain the most extensively studied techniques for active droplet transport and manipulation.

DEP is based on electromechanical forces exerted on electrically neutral liquids when the fluid is exposed to nonuniform electric fields; this results in the attraction of polarizable fluid toward regions with higher electric field intensity (104). In this case, the liquid must be of higher dielectric permittivity than the surrounding fluid. The primary forces involved with DEP are the wetting force on the interfacial line between the droplet, surrounding medium, and the contact surface; the force on the fluid interface; and the body force owing to the pressure gradient in the fluid (98). The liquid profile is dependent on the frequency of the applied field. Below the critical frequency, given by

$$f_c = \frac{G_w}{2\pi(C_d/2 + C_w)}, \quad 10.$$

where G_w is the conductance, C_d is the dielectric coating, and C_w is the capacitance, the entire voltage drop occurs across the dielectric layer, and the liquid becomes equipotential and wets the entire electrode surface. Above the critical frequency, only some portion of the total applied voltage drop occurs in the water and, as a result, the liquid remains in drop form (107). By manipulating the frequency and magnitude of the applied voltage, the size and uniformity of the droplets can be controlled.

In contrast, EWOD-based droplet platforms apply an electric field to reduce the solid-liquid interfacial energy, rendering the solid surface hydrophilic and enhancing the surface's wettability (108). This correspondence between the solid-liquid interfacial tension, γ_{SL}, and the applied voltage, V, is shown by Lippmann's equation,

$$\gamma_{SL} = \gamma_{SL}^0 - \frac{\varepsilon V^2}{2d}, \quad 11.$$

where γ_{SL}^0 is the interfacial tension at zero applied potential and ε and d are the dielectric constant and thickness of the insulating film, respectively (109). The droplet formation process is initiated as a series of adjacent electrodes are actuated and a liquid protrusion is formed; when intermediate electrodes are sequentially grounded, these surfaces revert back to their hydrophobic state, forming a droplet from the contained fluid. With this mechanism, the strength and frequency of the applied electric field and the width of the channel determine the resultant droplet size.

Reagent Addition and Mixing

Conducting a chemical assay in a microfluidic droplet often requires addition or fusion of picoliter to nanoliter volumes of reagents to initiate reactions (**Figure 5*a*,*b***). The mechanism for passive droplet fusion involves three steps: (*a*) droplet collision, (*b*) film drainage, and (*c*) film rupture. The rate and efficiency of droplet coalescence depend on the fluid drainage dynamics near the contact regions between the droplet interfaces (110) and surfactants that stabilize emulsions by increasing deformation and causing surface tension gradients (111). The drainage dynamics can be controlled by adjusting the fluid flow rate, droplet generation frequency, and channel design, with higher rates of film drainage increasing the coalescence rate (110, 112). Furthermore, the rate of film drainage is dependent on the viscosity ratio of the two fluids and the surfactant at the fluid interface (113). Higher viscosity ratios render the interfaces less mobile, and surfactants stabilize droplets thereby reducing coalescence events (114). Surfactant effects are determined by the Marangoni number, which is the ratio of surface tension forces to viscous forces. When the Marangoni number, $Mg = E/Ca$, where E is the Gibbs-Marangoni elasticity, exceeds a critical value, the interface is saturated with surfactant, and further increase of surfactant concentration has no influence on coalescence (113).

Droplets can also be fused actively with electric, magnetic, thermal, or optical mechanisms (**Figure 5*c***). In DEP fusion, the droplet composition must be dielectrically distinct from that of its carrier fluid for the drop to become polarized. Typical operation involves activating an electrode adjacent to the target droplets to guide neighboring droplets toward the region with higher electric field. Coalescence in this central region occurs in a fashion similar to that in passive fusion techniques (98). On one hand, unstabilized droplets will spontaneously fuse, reducing the system's entropy and surface energy. Stabilized droplets, on the other hand, may not spontaneously fuse;

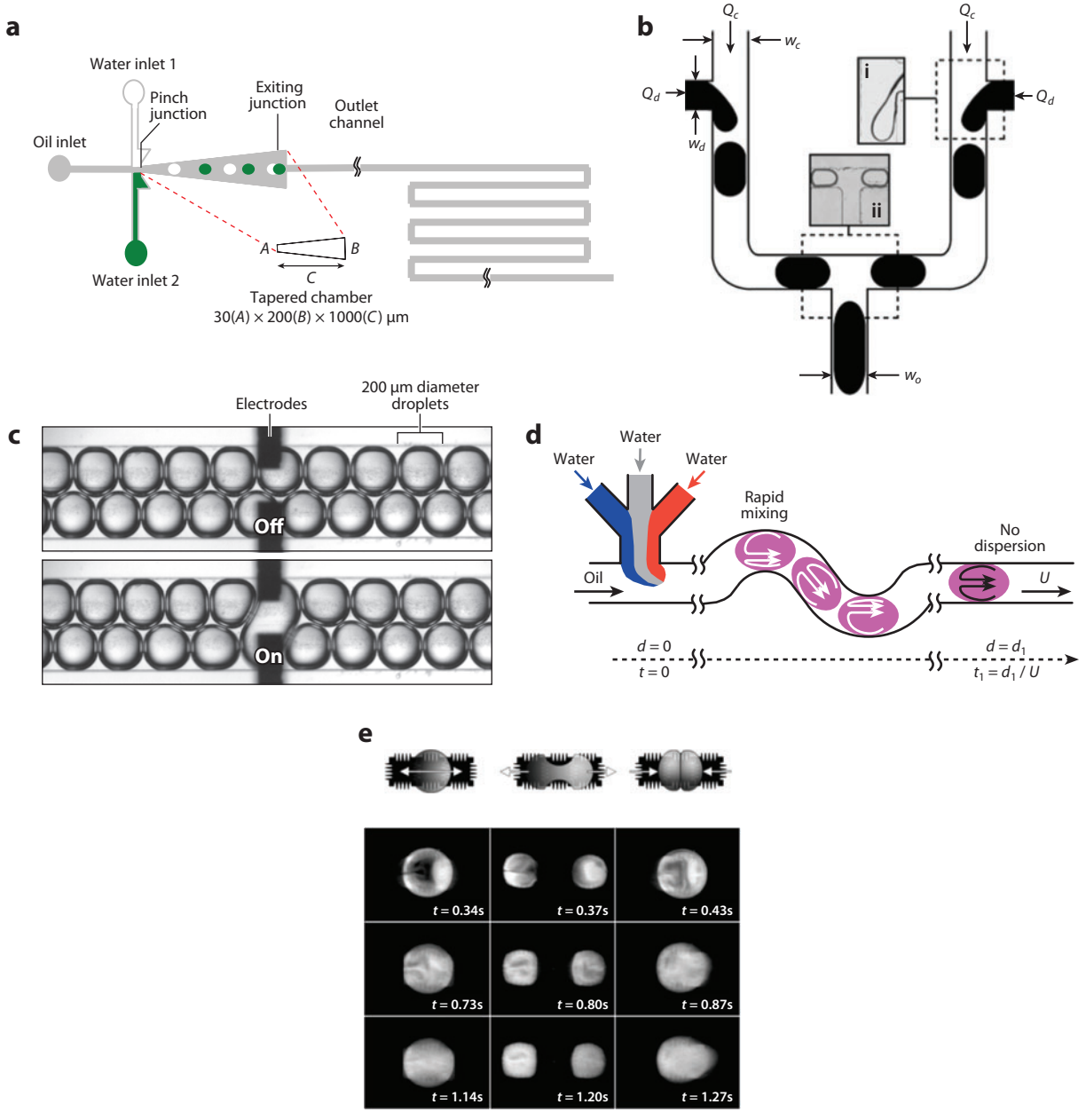

electrical pulses or larger voltages are sometimes needed to induce coalescence (115, 116). Non-electrical means, e.g., magnetic beads (117) or optical tweezers (118), have also been demonstrated as fusion mechanisms. Magnetic particles can be used to bring two droplets together until fusion occurs (117). Optical tweezers also offer precise control and accuracy for fusion events but have limitations owing to their complicated and expensive setup (118).

Once reagents are fused with sample droplets, the slow mixing times inherent in laminar flow systems require careful design to encourage on-chip mixing. Without convection, the contents of fused droplets will remain segregated, mixing only by molecular diffusion (119). In mass transfer, the diffusion mixing time can be approximated by $t_{\text{diff}} = \frac{s_0^2}{D}$, where s_0 is the initial striation length and D is the diffusion coefficient. As a result, convective flow and chaotic advection have been used in passive systems to reduce the mixing time by essentially reducing striation length (120) (**Figure 5*d***). For a droplet traversing a straight channel, there exists a critical velocity,

$$V_c = \pi^2 \left(\frac{L}{d}\right)\left(\frac{D}{d}\right), \qquad 12.$$

where L is the droplet length, D is the solute diffusivity, and d is the microchannel depth, above which convection-based mixing dominates and below which diffusion-based mixing dominates (121, 122). Convective mixing is preferred, and complete mixing can occur in fractions of a second as long as the drop traverses at least 3–5 drop lengths (123). Chaotic advection, in which unsteady fluid flow is formed as the droplets move through winding channels, works on a similar principle: The drop motion results in an exponential decrease in the striation length (120, 124), and the mixing time, $t_{\text{mix,ca}}$, is proportional to the time scale for convective transport. In particular,

$$t_{\text{mix,ca}} \sim \left(\frac{a\,w}{U}\right)\log(Pe), \qquad 13.$$

where a is the dimensionless length of the plug relative to the width, w, and U is the flow velocity (124). Chaotic advection has been reported to reduce mixing time significantly, as the winding channels cause droplets to undergo the baker's transformation (i.e., the droplets are stretched, folded, and reoriented) (124, 125).

When passive mixing techniques are not sufficient, active mixing methods can be used. Active techniques, which are predominantly electrically controlled, provide benefits over passive techniques because mixing occurs in more confined regions and mixing in a single droplet can be controlled (**Figure 5*e***). Rapid oscillation-based mixing is achieved through controlling the charge of neighboring electrodes which causes the substrate surface to wet and dewet sequentially (126).

Figure 5

Droplet fusion and mixing using passive and active mechanisms. Droplets can be passively fused via two mechanisms. (*a*) Adjust the channel geometry and size (*A*, *B*, *C*) to reduce the liquid flow rate such that two droplets come into contact and fuse. Reproduced with permission from Reference 110, copyright © 2006, The Royal Society of Chemistry. (*b*) Adjust the flow rate to instigate droplet collision and fusion events. Q_c, flow rate of continuous phase; Q_d, flow rate of disperse phase; w, channel width. Inset *i* shows droplet formation at the T-junction, and inset *ii* shows how the resultant droplet streams interact at the downstream T-junction. Reproduced with permission from Reference 112, copyright © 2009, The Royal Society of Chemistry. Droplets can also be actively fused by (*c*) applying an electric field potential across two adjacent droplets, which causes instability at the oil/water interface, inducing fusion. Reprinted with permission from Reference 115, copyright © 2006, American Institute of Physics. (*d*) Rapid mixing techniques in passive systems can be accomplished by flowing droplets through winding channels, which change the internal circulation flow patterns; *d*, distance; *t*, time; *U*, flow rate (120). Copyright © Wiley-VCH Verlag GmbH & Co. KGaA. Reproduced with permission. (*e*) With the use of electrodes, droplets can be actively mixed by rapidly adjusting the hydrophilic property of neighboring electrodes, which causes the droplet to shift back and forth, or by sequential droplet splitting and merging. Reproduced with permission from Reference 127, copyright © 2003, The Royal Society of Chemistry.

Splitting and merging techniques often utilize a three-electrode system. Droplets are split when current is applied to neighboring electrodes and the central electrode is grounded; however, when the central electrode is activated and the neighboring electrodes deactivated, the droplets will again merge (127). Finally, a linear and planar array method can be used to introduce bidirectional fluid motion in the droplet (127, 128).

Reactions and Postprocessing

The ability to fuse and mix large quantities of droplets in microfluidic devices enables large-scale, parallel assay reactions to be performed. Each droplet behaves as a separate microreaction chamber; the number of reactions depends on the quantity of droplets that can be isolated in each channel or chamber. By arranging droplets in array formats within channels (105) or microarray plates (129), parallel reactions can be conducted with varying reagent types or concentrations. Reactions, such as those in PCR, enzyme assays, or cell-based assays, require thermal modulation. As a result, resistive heaters and temperature sensors have been fabricated on-chip to control the temperature of the system locally (11), or external heating elements can be incorporated to control the temperature of larger systems (102).

After the reactions have taken place, the products within the droplet may need to be purified, or the droplet itself may need to be split into smaller droplets for further analysis (**Figure 6*a*,*b***). Additionally, the initial droplet may need to be split into smaller droplets for parallel assay applications or for controlling content concentrations (130). Passive droplet fission techniques include the use of T-junctions, branching channels, or channel obstructions. Passive fission techniques in T-junctions are governed by the *Ca* number (see **Table 2**), the viscosity ratio η_1/η_2, and the flow rate ratio Q_1/Q_2, where η is the viscosity and Q is the flow rate (131). The relative size of the daughter droplets is precisely controlled through one or more of these variables. Droplet fission in microchannels was first demonstrated by constricting the channel dimensions at the branching point (T-junction), having the droplet elongate into both of the daughter channels, and then continuing the flow of the continuous phase until droplet fission occurred (120). For other T-junction-based systems, the relative sizes of the daughter droplets can be controlled by modulating the relative resistances of the side channels and the flow rates of both the dispersed and continuous phases. In this case, the formation of identically sized daughter droplets at the T-junction is governed by the critical capillary number,

$$Ca_{cr} = \alpha\varepsilon_0 \left(\frac{1}{\varepsilon_0^{2/3}} - 1 \right)^2, \qquad 14.$$

where α is a dimensionless constant that is a function of the viscosity difference of the two fluids and the geometry of the channel, and ε_0 is the ratio of initial droplet length to initial droplet circumference (132). In addition, droplet splitting and the resulting sizes of the daughter droplets can be controlled through the strategic placement of a channel obstruction (98).

As with all operations, droplet fission can be controlled actively, with electrical, magnetic, or thermal control. The concept of droplet fission is essentially identical to that of droplet formation because both processes involve separating one liquid entity from another. For instance, in EWOD, electrodes on opposite ends of the droplet are activated to reduce the liquid-surface interfacial energy so that the droplet wets the surface; upon removal of the field from the central electrode, the central region is rendered hydrophobic, separating the droplets (133). Magnet-based mechanisms have also been used; for instance, magnetic particles inside a droplet can be actuated to separate, thus entraining fluid and splitting the drop (117). Droplets also can be split by thermal actuation,

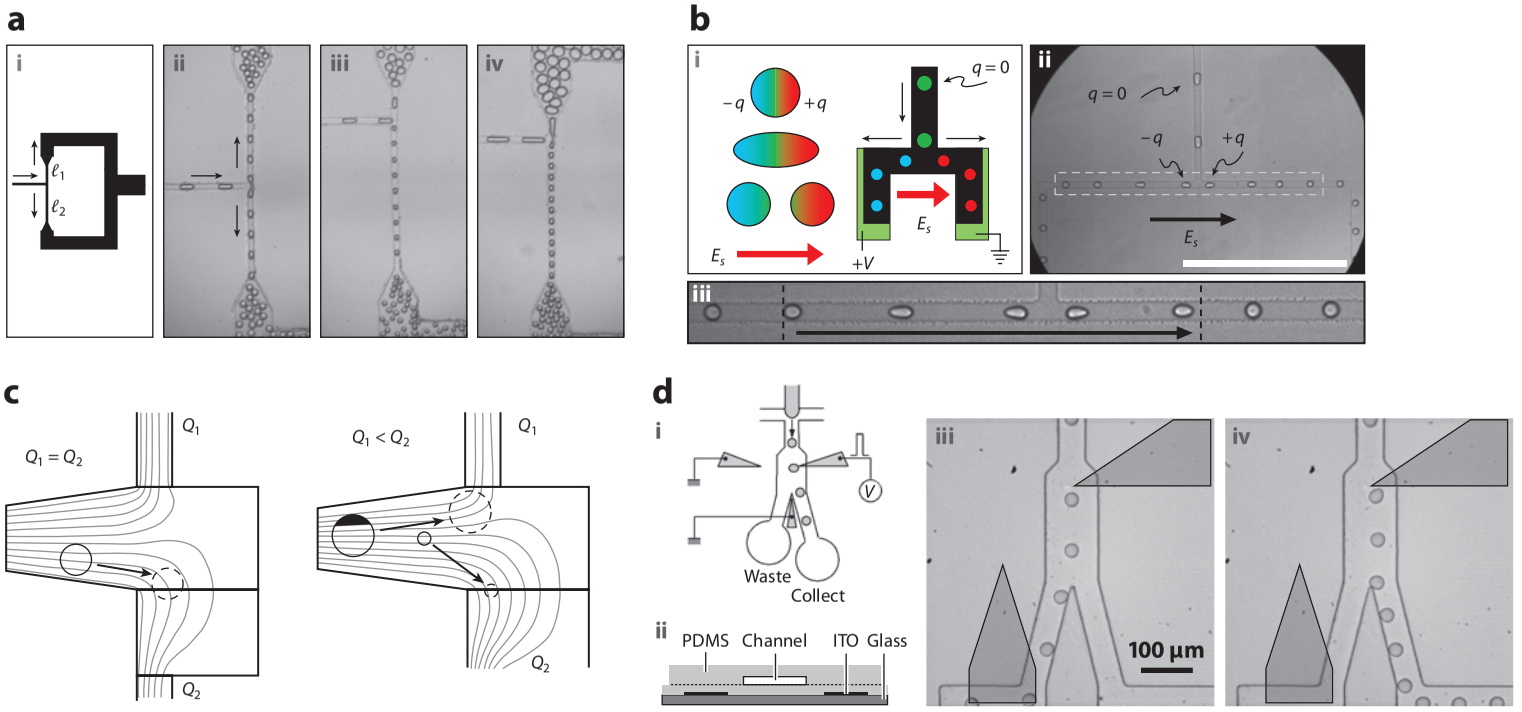

Figure 6

Droplet fission and sorting mechanisms can be controlled both passively and actively. (*a*) The most common passive fission technique is to drive a droplet at sufficient flow rates into a T-junction. By adjusting the flow resistance patterns on the daughter channels (ℓ is the respective channel length), the sizes of the daughter droplets can be controlled. Reproduced with permission from Reference 132, copyright © 2004, American Physical Society. (*b*) The droplets can also be split according to the droplet content using an active sorting and passive fission technique. A voltage (V) is applied, which generates a signal electric field (E_s) that will cause the contents to polarize, and upon droplet fission, the daughter droplets will be sorted by the electrical potential (q) of their contents (135). Copyright © Wiley-VCH Verlag GmbH & Co. KGaA. Reproduced with permission. (*c*) Size-based sorting can be achieved using passive mechanisms, as the size and location of the droplet and flow pattern at the T-junction region determines its sorting behavior. Q, flow rate. Reproduced with permission from Reference 130, copyright © 2004, The Royal Society of Chemistry. (*d*) Droplets can be actively sorted using electric fields by applying a voltage (V) at an electrode, which causes the drops to be attracted to the activated electrode. By sequentially activating and grounding the electrode, target droplets can be selectively sorted from waste droplets. PDMS, polydimethylsiloxane; ITO, indium-tin-oxide. Reprinted with permission from Reference 137, copyright © 2006, American Institute of Physics.

in which neighboring sides of the droplet are heated, reducing the viscosity and lowering the interfacial tension of the outer edges of the droplets. As a result, the droplets naturally veer toward regions of higher temperature (131)—this phenomenon is akin to the motion of droplets in hydrophobic environments toward regions of higher temperature (26). By strategically heating certain regions in the microfluidic channels, such as one of the daughter channels of a T-junction system, unevenly sized droplets can result from the fission process.

Droplet sorting is highly advantageous to control droplet volume for fission or fusion processes, or for selectively enriching specific droplet subpopulations (**Figure 6*c*,*d***). Passive sorting most commonly uses size-based techniques that control the flow rate and flow geometry (130, 134). For example, size-based sorting can be used to remove residual or satellite droplets created during the droplet formation process, thus increasing the monodispersity of the subpopulation (130). Sorting based solely on size does not find many applications in biochemical assays as content-based sorting is desired. However, in cases in which droplet content correlates directly with droplet size, such as cell encapsulation, passive sorting mechanisms may be used to sort empty and cell-occupied droplets (134).

Content-based sorting is more commonly achieved with active mechanisms such as sensors, actuators, and valves. Recently, nonmechanical active sorting mechanisms have been developed that separate target droplets with electric fields (135) or localized heating (136). DEP-based sorting techniques use electric fields to electrostatically charge the droplets and guide them into their designated downstream channels through steering or deflection mechanisms (135, 137). The degree of control is determined by the field gradient generated, which depends on the electrode location and shape (98). Using DEP, droplets can be sorted according to fluorescent content; droplets are categorized by their fluorescence intensity, and target droplets are separated by a pulse of high-voltage AC emitted across electrodes adjacent to the sorting channel (138). Although not as common as DEP-based sorting, EWOD sorting is achieved by selectively changing the interfacial energy between the droplet and the surface to split the droplet. This driving mechanism for droplet splitting can be applied to electrophoresis; as a result, the contents of the droplets can be sorted and split sequentially (133). Another technique uses localized heating, which generates thermocapillary flow such that the heating increases the surface tension, which is the case in the presence of specific surfactants, providing a blocking force to halt or diverge droplet flow (136).

Complex Integrated Systems

One of the main advantages of microfluidic systems in general and droplet microfluidic systems specifically is that many different operations can be combined within a single device, allowing the construction of complex assays (**Figure 7**). The aim of these systems is to develop lab-on-a-chip

Figure 7

Complex integrative systems incorporate multiple droplet control techniques for unique chemical assay applications. (*a*) A highly integrative droplet device that incorporates droplet mixing, thermal cycling, gel electrophoresis, and fluorescent detectors to analyze nanoliter-sized DNA samples. From Reference 139. Reprinted with permission from AAAS. (*b*) Droplets can be rapidly sorted when an alternating current electric field is applied across the adjacent electrodes, deflecting the droplets into the upper channel. In the absence of the field, the droplets flow into the lower channel (*inset on right image*). The activation of the AC electric field is determined upstream by a fluorescence detector; therefore, target droplets that exhibit fluorescence above a baseline level will be deflected to the upper channel. Reproduced with permission from Reference 138, copyright © 2009, The Royal Society of Chemistry. (*c*) A user-loaded, equipment-free SlipChip allows for multiplex performance of nanoliter-scale experiments by combining a sample with multiple reagent types at multiple mixing ratios. SlipChip has been demonstrated in protein crystallization applications but is applicable to enzyme kinetics studies, cell-based assays, and chemical reactions. Reproduced with permission from Reference 141, copyright © 2010, American Chemical Society.

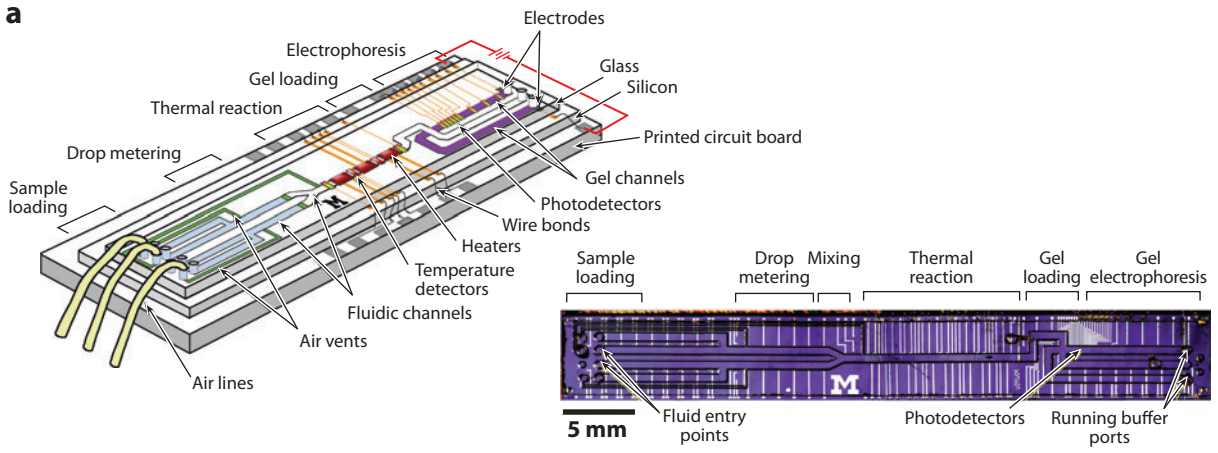

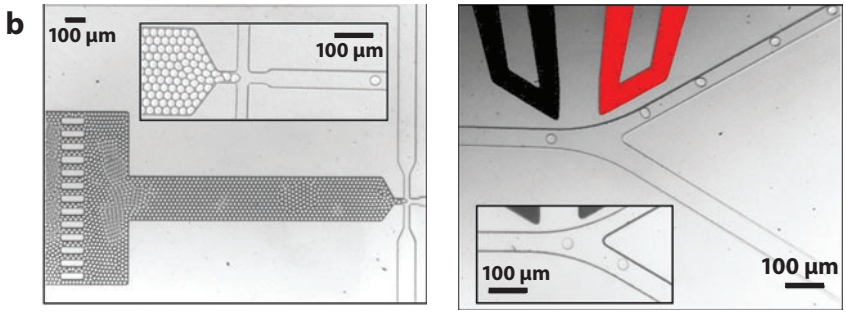

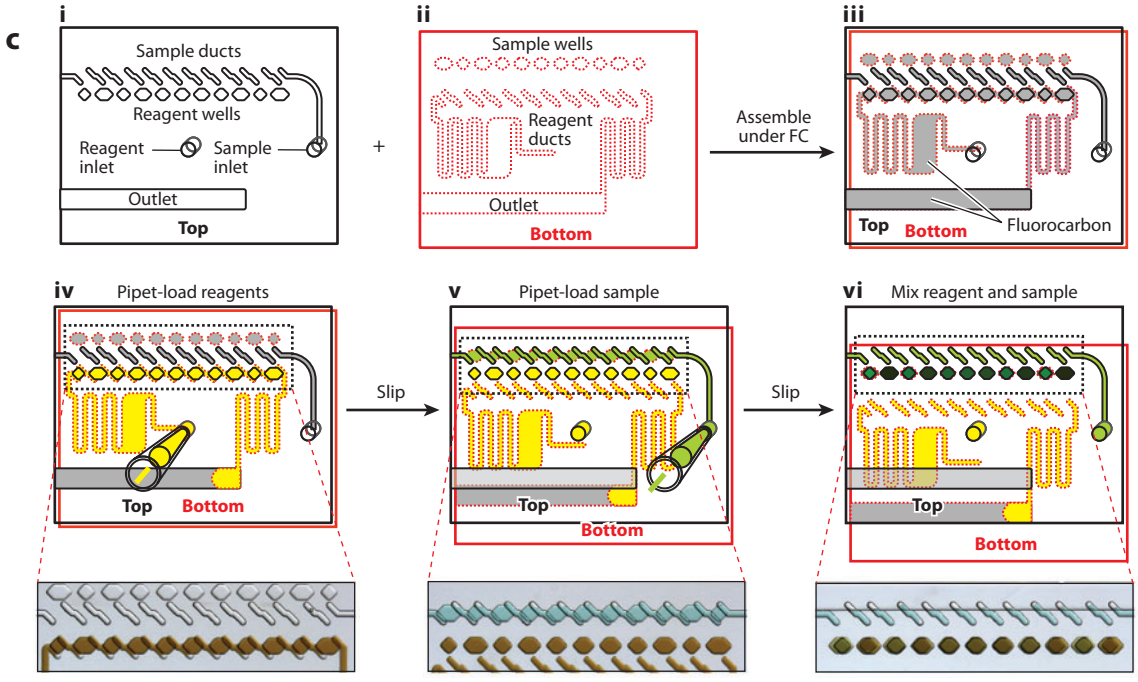

devices that perform many operations including sequential sample preparation, reaction, detection, and analysis in a single device. However, even though such devices are theoretically possible, the commercialization and widespread development of these fully integrated and automated systems are still largely in the future. Integrating components into a single system significantly increases the difficulty of system design and operation compared with single-component systems.

One of the first highly integrated droplet microfluidic analysis systems consisting of fluidic channels, heaters, temperature sensors, and fluorescence detectors was developed in 1998 (139). The device required minimal external equipment (several air lines to initiate drop motion, an LED for fluorescent excitation, and power/computer connections) and did not require external optics (e.g., a microscope), valves, heaters, or pumps. Aqueous reagents could be sequentially metered and dispensed, solutions mixed, DNA amplified, and products separated and detected. This system allowed for smaller samples and increased detection speeds as compared with conventional systems, but was limited as it lacked on-chip sample preparation and used uncommon reaction protocols [i.e., strand displacement amplification (SDA)].

Current DNA analysis chips use the more common PCR because of the wide applicability of the reaction to clinically relevant assays (140). Conventional benchtop PCR is limited in that the large number of preparation steps often results in sample loss and contamination (102). Significant advancement toward complete lab-on-a-chip PCR technology has been made with the integration of on-chip thermal cyclers, electrophoresis, and detection (139). However, these highly integrated systems lack the ability to run multiple reactions in parallel. A recently developed droplet-based microfluidic device integrates sample preparation and PCR analysis as well as the ability to process multiple samples in parallel in a semiautomated fashion (140). Current research in this field focuses on the optimization of a fully integrated PCR device, the development of automated control systems, and the ability to conduct single-cell analysis PCR studies with high throughput and sensitivity (102).

Droplet microfluidic technology is also used for enzyme assays and chemical reaction analysis, as isolated reactions can be conducted concurrently at high throughput. Recently, there has been interest in developing multiplexed kinetic reaction systems to study chemically diverse samples; in this case, many droplets containing different ratios or types of reagent or solution can be chemically analyzed in parallel. With an automated technique to fuse samples with reagents at multiple mixing ratios, large-scale screening assays for enzymatic, drug-discovery, or crystallization studies would be possible (141). Screening times can be further reduced if detection methods that monitor the reaction kinetics in array systems or in constant flow conditions are incorporated and automated (142, 143).

FUTURE OUTLOOK

Microfluidic systems have the capability to replace many conventional macroscale systems because of their low consumption of reagents and samples, ability to manipulate small volumes with ease, and high speed of reactions and separations. Furthermore, processes in microfluidic systems are conducted at scales more relevant to biological conditions (e.g., the volume of a single cell), and highly parallel chips processing large numbers of samples can be constructed easily (144). In recent years, there has been significant advancement in the development and implementation of high-density microfluidic chips for a diverse range of applications in biological and chemical analysis, and in the diagnosis and treatment of diseases (145). The general trend continues toward a μTAS in which the system performs sampling, sample preparation and transport, chemical reactions, and detection in a single, miniaturized platform (146). Specifically, interest is escalating in using microfluidics for biosensing applications, for single-molecule or single-cell detection and

analysis, and for the development of inexpensive, portable diagnostics that can be implemented in developing countries for personal care (145).

Although the size of typical microfluidic channels is quite small (typically 10–500 μm in diameter) there is significant interest in devices with even smaller dimensions, which has resulted in the rapid emergence of nanofluidics, the study of fluidic transport at the nanometer scale. In nanometer-sized channels, individual macromolecules such as DNA can be trapped and studied (147). This steady decrease in dimensions approaches the limit of the continuum approximation at which the Navier-Stokes equations break down. However, for water under normal conditions, the continuum hydrodynamic limit remains robust down to dimensions of tens of nanometers; thus, the Navier-Stokes equation remains accurate in most of these situations (148). Therefore, the unique aspects of nanofluidics center on the study of surface effects not apparent at the micrometer scale.

Despite significant advances in the young field of microfluidics, there remain limitations to the widespread commercialization of this technology mainly because of economic considerations. PDMS lithography and other material advances have significantly reduced the cost of microfluidic substrates, but this may be only a fraction of the total cost. The cost of electronic chips typically scales with the number of separate lithography steps (i.e., mask sets), and the same holds true for microfluidic systems (149). In addition, multiple materials in the final device (e.g., laminations, valve material), reagent addition to and storage on the chip, packaging of the final device, and micro-macro connections with computers and/or fluidic control systems all add to the cost of the assay system. Nevertheless, microfluidics possesses enormous potential, and the extensive worldwide research to develop and commercialize fully automated and integrated systems will most likely result in a wide variety of bioanalysis applications in the not too distant future.

DISCLOSURE STATEMENT

The authors are not aware of any affiliations, memberships, funding, or financial holdings that might be perceived as affecting the objectivity of this review.

LITERATURE CITED

1. Whitesides GM. 2006. The origins and the future of microfluidics. *Nature* 442(7101):368–73
2. Stone HA, Kim S. 2001. Microfluidics: basic issues, applications, and challenges. *AIChE J.* 47(6):1250–54
3. Tabeling P. 2005. *Introduction to Microfluidics*. New York: Oxford Univ. Press
4. Reyes DR, Iossifidis D, Auroux P, Manz A. 2002. Micro total analysis systems. 1. Introduction, theory, and technology. *Anal. Chem.* 74(12):2623–36
5. Sundberg SA. 2000. High-throughput and ultra-high-throughput screening: solution- and cell-based approaches. *Curr. Opin. Biotechnol.* 11(1):47–53
6. Nguyen N, Wereley ST. 2002. *Fundamentals and Applications of Microfluidics*. Boston, MA: Artech House
7. Bruus H. 2008. *Theoretical Microfluidics*. New York: Oxford Univ. Press
8. Squires TM, Quake SR. 2005. Microfluidics: fluid physics at the nanoliter scale. *Rev. Mod. Phys.* 77(3):977–1026
9. Purcell EM. 1977. Life at low Reynolds number. *Am. J. Phys.* 45(1):3–11
10. deMello AJ. 2006. Control and detection of chemical reactions in microfluidic systems. *Nature* 442(7101):394–402
11. Pal R, Yang M, Lin R, Johnson BN, Srivastava N, et al. 2005. An integrated microfluidic device for influenza and other genetic analyses. *Lab. Chip* 5(10):1024–32
12. Thorsen T, Maerkl SJ, Quake SR. 2002. Microfluidic large-scale integration. *Science* 298(5593):580–84
13. Lee BS, Lee J, Park J, Lee J, Kim S, et al. 2009. A fully automated immunoassay from whole blood on a disc. *Lab. Chip* 9(11):1548–55

14. Kong J, Jiang L, Su X, Qin J, Du Y, Lin B. 2009. Integrated microfluidic immunoassay for the rapid determination of clenbuterol. *Lab. Chip* 9(11):1541–47
15. Fan R, Vermesh O, Srivastava A, Yen BKH, Qin L, et al. 2008. Integrated barcode chips for rapid, multiplexed analysis of proteins in microliter quantities of blood. *Nat. Biotechnol.* 26(12):1373–78
16. Lashkari DA, Derisi JL, McCusker JH, Namath AF, Gentile C, et al. 1997. Yeast microarrays for genome wide parallel genetic and gene expression analysis. *Proc. Natl. Acad. Sci. USA* 94:13057–62
17. Jorgenson JW, Lukacs KDA. 1983. Capillary zone electrophoresis. *Science* 222(4621):266–72
18. Huang X, Gordon MJ, Zare RN. 1988. Current-monitoring method for measuring the electroosmotic flow rate in capillary zone electrophoresis. *Anal. Chem.* 60(17):1837–38
19. Kirby BJ. 2010. *Micro- and Nanoscale Fluid Mechanics: Transport in Microfluidic Devices*. New York: Cambridge Univ. Press
20. Seller K, Fan ZH, Flurl K, Harrison DJ. 1994. Electroosmotic pumping and valveless control of fluid flow within a manifold of capillaries on a glass chip. *Anal. Chem.* 66(20):3485–91
21. Ocvirk G, Munroe M, Tang T, Oleschuk R, Westra K, Harrison DJ. 2000. Electrokinetic control of fluid flow in native poly(dimethylsiloxane) capillary electrophoresis devices. *Electrophoresis* 21(1):107–15
22. Kittilsland G, Stemme G, Nordén B. 1990. A sub-micron particle filter in silicon. *Sens. Actuators A* 23(1–3):904–7
23. Inman W, Domansky K, Serdy J, Owens B, Trumper D, Griffith LG. 2007. Design, modeling and fabrication of a constant flow pneumatic micropump. *J. Micromech. Microeng.* 17(5):891–99
24. Laser DJ, Santiago JG. 2004. A review of micropumps. *J. Micromech. Microeng.* 14(6):R35–64
25. Juncker D, Schmid H, Drechsler U, Wolf H, Wolf M, et al. 2002. Autonomous microfluidic capillary system. *Anal. Chem.* 74(24):6139–44
26. Sammarco TS, Burns MA. 1999. Thermocapillary pumping of discrete drops in microfabricated analysis devices. *AIChE J.* 45(2):350–66
27. Srivastava N, Davenport RD, Burns MA. 2005. Nanoliter viscometer for analyzing blood plasma and other liquid samples. *Anal. Chem.* 77(2):383–92
28. Grushka E. 1991. Effect of hydrostatic flow on the efficiency in capillary electrophoresis. *J. Chromatogr. A* 559(1–2):81–93
29. Morier P, Vollet C, Michel PE, Reymond F, Rossier JS. 2004. Gravity-induced convective flow in microfluidic systems: electrochemical characterization and application to enzyme-linked immunosorbent assay tests. *Electrophoresis* 25(21–22):3761–68
30. Yao B, Luo G, Feng X, Wang W, Chen L, Wang Y. 2004. A microfluidic device based on gravity and electric force driving for flow cytometry and fluorescence activated cell sorting. *Lab. Chip* 4(6):603–7
31. Duffy DC, Gillis HL, Lin J, Sheppard NF Jr, Kellogg GJ. 1999. Microfabricated centrifugal microfluidic systems: characterization and multiple enzymatic assays. *Anal. Chem.* 71(20):4669–78
32. Takayama S, Ostuni E, LeDuc P, Naruse K, DE. 2003. Selective chemical treatment of cellular microdomains using multiple laminar streams. *Chem. Biol.* 10:123–30
33. Jeon NL, Baskaran H, Dertinger SKW, Whitesides GM, Van De Water L, Toner M. 2002. Neutrophil chemotaxis in linear and complex gradients of interleukin-8 formed in a microfabricated device. *Nat. Biotechnol.* 20(8):826–30
34. Jeon NL, Dertinger SKW, Chiu DT, Choi IS, Stroock AD, Whitesides GM. 2000. Generation of solution and surface gradients using microfluidic systems. *Langmuir* 16(22):8311–16
35. Dertinger SKW, Chiu DT, Jeon NL, Whitesides GM. 2001. Generation of gradients having complex shapes using microfluidic networks. *Anal. Chem.* 73(6):1240–46
36. Amarie D, Glazier JA, Jacobson SC. 2007. Compact microfluidic structures for generating spatial and temporal gradients. *Anal. Chem.* 79(24):9471–77
37. Oddy MH, Santiago JG, Mikkelsen JC. 2001. Electrokinetic instability micromixing. *Anal. Chem.* 73(24):5822–32
38. Hertzog DE, Ivorra B, Mohammadi B, Bakajin O, Santiago JG. 2006. Optimization of a microfluidic mixer for studying protein folding kinetics. *Anal. Chem.* 78(13):4299–306
39. Handique K, Gogoi BP, Burke DT, Mastrangelo CH, Burns MA. 1997. Microfluidic flow control using selective hydrophobic patterning. *Proc. SPIE* 3224:185–195

40. Johnson TJ, Ross D, Locascio LE. 2002. Rapid microfluidic mixing. *Anal. Chem.* 74(1):45–51
41. Hawkins KR, Steedman MR, Baldwin RR, Fu E, Ghosal S, Yager P. 2007. A method for characterizing adsorption of flowing solutes to microfluidic device surfaces. *Lab. Chip* 7(2):281–85
42. Unger MA, Chou H, Thorsen T, Scherer A, Quake SR. 2000. Monolithic microfabricated valves and pumps by multilayer soft lithography. *Science* 288(5463):113–16
43. Grover WH, Skelley AM, Liu CN, Lagally ET, Mathies RA. 2003. Monolithic membrane valves and diaphragm pumps for practical large-scale integration into glass microfluidic devices. *Sens. Actuators B* 89(3):315–23
44. Hasselbrink, Shepodd TJ, Rehm JE. 2002. High-pressure microfluidic control in lab-on-a-chip devices using mobile polymer monoliths. *Anal. Chem.* 74(19):4913–18
45. Pal R, Yang M, Johnson BN, Burke DT, Burns MA. 2004. Phase change microvalve for integrated devices. *Anal. Chem.* 76(13):3740–48
46. Woolley AT, Hadley D, Landre P, DeMello AJ, Mathies RA, Northrup MA. 1996. Functional integration of PCR amplification and capillary electrophoresis in a microfabricated DNA analysis device. *Anal. Chem.* 68(23):4081–86
47. Andersson H, van der Wijngaart W, Enoksson P. 2000. Micromachined flow-through filter-chamber for chemical reactions on beads. *Sens. Actuators B* 67(1–2):203–8
48. Sia SK, Whitesides GM. 2003. Microfluidic devices fabricated in poly(dimethylsiloxane) for biological studies. *Electrophoresis* 24(21):3563–76
49. Krishnamoorthy G, Carlen ET, Bomer JG, Wijnperlé D, deBoer HL, et al. 2010. Electrokinetic label-free screening chip: a marriage of multiplexing and high throughput analysis using surface plasmon resonance imaging. *Lab. Chip* 10(8):986–90
50. Wang Y, Stevens AL, Han J. 2005. Million-fold preconcentration of proteins and peptides by nanofluidic filter. *Anal. Chem.* 77(14):4293–99
51. Lin R, Burke DT, Burns MA. 2005. Addressable electric fields for size-fractioned sample extraction in microfluidic devices. *Anal. Chem.* 77(14):4338–47
52. Fu AY, Chou H, Spence C, Arnold FH, Quake SR. 2002. An integrated microfabricated cell sorter. *Anal. Chem.* 74(11):2451–57
53. Huang LR, Cox EC, Austin RH, Sturm JC. 2004. Continuous particle separation through deterministic lateral displacement. *Science* 304(5673):987–90
54. Panaro NJ, Lou XJ, Fortina P, Kricka LJ, Wilding P. 2005. Micropillar array chip for integrated white blood cell isolation and PCR. *Biomol. Eng.* 21(6):157–62
55. Morton KJ, Loutherback K, Inglis DW, Tsui OK, Sturm JC, et al. 2008. Crossing microfluidic streamlines to lyse, label and wash cells. *Lab. Chip* 8(9):1448–53
56. Norris JV, Evander M, Horsman-Hall KM, Nilsson J, Laurell T, Landers JP. 2009. Acoustic differential extraction for forensic analysis of sexual assault evidence. *Anal. Chem.* 81(15):6089–95
57. MacDonald MP, Spalding GC, Dholakia K. 2003. Microfluidic sorting in an optical lattice. *Nature* 426(6965):421–24
58. El-Ali J, Sorger PK, Jensen KF. 2006. Cells on chips. *Nature* 442(7101):403–11
59. Dishinger JF, Kennedy RT. 2007. Serial immunoassays in parallel on a microfluidic chip for monitoring hormone secretion from living cells. *Anal. Chem.* 79(3):947–54
60. Hung PJ, Lee PJ, Sabounchi P, Lin R, Lee LP. 2005. Continuous perfusion microfluidic cell culture array for high-throughput cell-based assays. *Biotechnol. Bioeng.* 89(1):1–8
61. Park ES, Brown AC, DiFeo MA, Barker TH, Lu H. 2010. Continuously perfused, non-cross-contaminating microfluidic chamber array for studying cellular responses to orthogonal combinations of matrix and soluble signals. *Lab. Chip* 10(5):571–80
62. Chapin SC, Pregibon DC, Doyle PS. 2009. High-throughput flow alignment of barcoded hydrogel microparticles. *Lab. Chip* 9(21):3100–9
63. Leclerc E, David B, Griscom L, Lepioufle B, Fujii T, et al. 2006. Study of osteoblastic cells in a microfluidic environment. *Biomaterials* 27(4):586–95
64. Kulesh DA, Clive DR, Zarlenga DS, Greene JJ. 1987. Identification of interferon-modulated proliferation-related cDNA sequences. *Proc. Natl. Acad. Sci. USA* 84(23):8453–57

65. Battifora H. 1986. The multitumor (sausage) tissue block: novel method for immunohistochemical antibody testing. *Lab. Investig.* 55(2):244–48
66. Kononen J, Bubendorf L, Kallionimeni A, Barlund M, Schraml P, et al. 1998. Tissue microarrays for high-throughput molecular profiling of tumor specimens. *Nat. Med.* 4(7):844–47
67. MacBeath G, Schreiber SL. 2000. Printing proteins as microarrays for high-throughput function determination. *Science* 289:1760–63
68. Ekins RP. 1998. Ligand assays: from electrophoresis to miniaturized microarrays. *Clin. Chem.* 44(9):2015–30
69. Zhu H, Bilgin M, Bangham R, Hall D, Casamayor A, et al. 2001. Global analysis of protein activities using proteome chips. *Science* 293(5537):2101–5
70. Tian J, Gong H, Sheng N, Zhou X, Gulari E, et al. 2004. Accurate multiplex gene synthesis from programmable DNA microchips. *Nature* 432:1050–54
71. Shingara J, Keiger K, Shelton J, Laosinchai-Wolf W, Powers P, et al. 2005. An optimized isolation and labeling platform for accurate microRNA expression profiling. *RNA* 11(9):1461–70
72. Gosalia DN, Diamond SL. 2003. Printing chemical libraries on microarrays for fluid phase nanoliter reactions. *Proc. Natl. Acad. Sci. USA* 100(15):8721–26
73. Eid J, Fehr A, Gray J, Luong K, Lyle J, et al. 2009. Real-time DNA sequencing from single polymerase molecules. *Science* 323(5910):133–38
74. Drmanac R, Sparks AB, Callow MJ, Halpern AL, Burns NL, et al. 2010. Human genome sequencing using unchained base reads on self-assembling DNA nanoarrays. *Science* 327(5961):78–81
75. Fodor SP, Read JL, Pirrung MC, Stryer L, Lu AT, Solas D. 1991. Light-directed, spatially addressable parallel chemical synthesis. *Science* 251(4995):767–73
76. Chee M, Yang R, Hubbell E, Berno A, Huang XC, et al. 1996. Accessing genetic information with high-density DNA arrays. *Science* 274(5287):610–14
77. Zammatteo N, Jeanmart L, Hamels S, Courtois S, Louette P, et al. 2000. Comparison between different strategies of covalent attachment of DNA to glass surfaces to build DNA microarrays. *Anal. Biochem.* 280(1):143–50
78. Barczak A, Rodriguez MW, Hanspers K, Koth LL, Tai YC, et al. 2003. Spotted long oligonucleotide arrays for human gene expression analysis. *Genome* 13:1775–85
79. Lam SH, Mathavan S, Gong Z. 2009. Zebrafish spotted-microarray for genome-wide expression profiling experiments. Part I: array printing and hybridization. *Methods Mol. Biol.* 546:175–95
80. Heller MJ. 2002. DNA microarray technology: devices, systems, and applications. *Annu. Rev. Biomed. Eng.* 4:129–53
81. Okamoto T, Suzuki T, Yamamoto N. 2000. Microarray fabrication with covalent attachment of DNA using bubble jet technology. *Nat. Biotechnol.* 18(4):438–41
82. Nam J, Thaxton CS, Mirkin CA. 2003. Nanoparticle-based bio-bar codes for the ultrasensitive detection of proteins. *Science* 301(5641):1884–86
83. Margulies M, Egholm M, Altman WE, Attiya S, Bader JS, et al. 2005. Genome sequencing in microfabricated high-density picolitre reactors. *Nature* 437(7057):376–80
84. Ronaghi M, Karamohamed S, Pettersson B, Uhlén M, Nyrén P. 1996. Real-time DNA sequencing using detection of pyrophosphate release. *Anal. Biochem.* 242(1):84–89
85. Mardis ER. 2008. Next-generation DNA sequencing methods. *Annu. Rev. Genomics Hum. Genet.* 9:387–402
86. Schena M, Shalon D, Heller R, Chai A, Brown PO, Davis RW. 1996. Parallel human genome analysis: microarray-based expression monitoring of 1000 genes. *Proc. Natl. Acad. Sci. USA* 93(20):10614–19
87. Eisen MB, Spellman PT, Brown PO, Botstein D. 1998. Cluster analysis and display of genome-wide expression patterns. *Proc. Natl. Acad. Sci. USA* 95(25):14863–68
88. Handl J, Knowles J, Kell DB. 2005. Computational cluster validation in post-genomic data analysis. *Bioinformatics* 21(15):3201–12
89. Tusher VG, Tibshirani R, Chu G. 2001. Significance analysis of microarrays applied to the ionizing radiation response. *Proc. Natl. Acad. Sci. USA* 98(9):5116–21

90. Zang S, Guo R, Zhang L, Lu Y. 2007. Integration of statistical inference methods and a novel control measure to improve sensitivity and specificity of data analysis in expression profiling studies. *J. Biomed. Inform.* 40(5):552–60
91. Zhang S. 2007. A comprehensive evaluation of SAM, the SAM R-package and a simple modification to improve its performance. *BMC Bioinform.* 8:230
92. Schena M, Shalon D, Davis RW, Brown PO. 1995. Quantitative monitoring of gene expression patterns with a complementary DNA microarray. *Science* 270(5235):467–70
93. Zhu H, Bilgin M, Bangham R, Hall D, Casamayor A, et al. 2001. Global analysis of protein activities using proteome chips. *Science* 293(5537):2101–5
94. Stewart KK. 1981. Flow-injection analysis: a review of its early history. *Talanta* 28(11):789–97
95. Rocks B, Riley C. 1982. Flow-injection analysis: a new approach to quantitative measurements in clinical chemistry. *Clin. Chem.* 28(3):409–21
96. Patton C, Crouch S. 1986. Experimental comparison of flow-injection analysis and air-segmented continuous flow analysis. *Anal. Chim. Acta* 179:189–201
97. Thorsen T, Roberts RW, Arnold FH, Quake SR. 2001. Dynamic pattern formation in a vesicle-generating microfluidic device. *Phys. Rev. Lett.* 86(18):4163–66
98. Teh S, Lin R, Hung L, Lee AP. 2008. Droplet microfluidics. *Lab. Chip* 8(2):198–220
99. Christopher GF, Anna SL. 2007. Microfluidic methods for generating continuous droplet streams. *J. Phys. D* 40(19):R319–36
100. Stone HA. 1994. Dynamics of drop deformation and breakup in viscous fluids. *Annu. Rev. Fluid Mech.* 26(1):65–102
101. Garstecki P, Fuerstman MJ, Stone HA, Whitesides GM. 2006. Formation of droplets and bubbles in a microfluidic T-junction-scaling and mechanism of break-up. *Lab. Chip* 6(3):437–46
102. Markey AL, Mohr S, Day PJ. 2010. High-throughput droplet PCR. *Methods* 50:277–81
103. Clausell-Tormos J, Lieber D, Baret J, El-Harrak A, Miller OJ, et al. 2008. Droplet-based microfluidic platforms for the encapsulation and screening of mammalian cells and multicellular organisms. *Chem. Biol.* 15(5):427–37
104. Song H, Chen DL, Ismagilov RF. 2006. Reactions in droplets in microfluidic channels. *Angew. Chem. Int. Ed.* 45(44):7336–56
105. Clausell-Tormos J, Griffiths AD, Merten CA. 2010. An automated two-phase microfluidic system for kinetic analyses and the screening of compound libraries. *Lab. Chip* 10(10):1302–7
106. Beyssen D, Le Brizoual L, Elmazria O, Alnot P. 2006. Microfluidic device based on surface acoustic wave. *Sens. Actuators B* 118(1–2):380–85
107. Jones TB, Gunji M, Washizu M, Feldman MJ. 2001. Dielectrophoretic liquid actuation and nanodroplet formation. *J. Appl. Phys.* 89(2):1441
108. Cho SK, Moon H, Kim C. 2003. Creating, transporting, cutting, and merging liquid droplets by electrowetting-based actuation for digital microfluidic circuits. *Microelectromech. Syst. J.* 12(1):70–80
109. Pollack MG, Shenderov AD, Fair RB. 2002. Electrowetting-based actuation of droplets for integrated microfluidics. *Lab. Chip* 2(2):96–101
110. Hung L, Choi KM, Tseng W, Tan Y, Shea KJ, Lee AP. 2006. Alternating droplet generation and controlled dynamic droplet fusion in microfluidic device for CdS nanoparticle synthesis. *Lab. Chip* 6(2):174–78
111. Cristini V, Tan YC. 2004. Theory and numerical simulation of droplet dynamics in complex flows—a review. *Lab. Chip* 4(4):257–64
112. Christopher GF, Bergstein J, End NB, Poon M, Nguyen C, Anna SL. 2009. Coalescence and splitting of confined droplets at microfluidic junctions. *Lab. Chip* 9(8):1102–9
113. Hudson SD, Jamieson AM, Burkhart BE. 2003. The effect of surfactant on the efficiency of shear-induced drop coalescence. *J. Colloid Interface Sci.* 265(2):409–21
114. Zheng B, Tice JD, Ismagilov RF. 2004. Formation of droplets of alternating composition in microfluidic channels and applications to indexing of concentrations in droplet-based assays. *Anal. Chem.* 76(17):4977–82
115. Priest C, Herminghaus S, Seemann R. 2006. Controlled electrocoalescence in microfluidics: targeting a single lamella. *Appl. Phys. Lett.* 89(13):134101

116. Schwartz JA, Vykoukal JV, Gascoyne PRC. 2004. Droplet-based chemistry on a programmable microchip. *Lab. Chip* 4(1):11–17
117. Lehmann U, Vandevyver C, Parashar VK, Gijs MAM. 2006. Droplet-based DNA purification in a magnetic lab-on-a-chip. *Angew. Chem. Int. Ed.* 45(19):3062–67
118. Lorenz RM, Edgar JS, Jeffries GDM, Chiu DT. 2006. Microfluidic and optical systems for the on-demand generation and manipulation of single femtoliter-volume aqueous droplets. *Anal. Chem.* 78(18):6433–39
119. Wang F, Burns MA. 2010. Droplet-based microsystem for multi-step bioreactions. *Biomed. Microdevices* 12(3):533–41
120. Song H, Tice JD, Ismagilov RF. 2003. A microfluidic system for controlling reaction networks in time. *Angew. Chem. Int. Ed.* 42(7):768–72
121. Handique K, Burns MA. 2001. Mathematical modeling of drop mixing in a slit-type microchannel. *J. Micromech. Microeng.* 11:548
122. Rhee M, Burns MA. 2008. Drop mixing in a microchannel for lab-on-a-chip platforms. *Langmuir* 24(2):590–601
123. Tice JD, Song H, Lyon AD, Ismagilov RF. 2003. Formation of droplets and mixing in multiphase microfluidics at low values of the Reynolds and the capillary numbers. *Langmuir* 19(22):9127–33
124. Song H, Bringer MR, Tice JD, Gerdts CJ, Ismagilov RF. 2003. Experimental test of scaling of mixing by chaotic advection in droplets moving through microfluidic channels. *Appl. Phys. Lett.* 83(22):4664–66
125. Stroock AD, Dertinger SKW, Ajdari A, Mezic I, Stone HA, Whitesides GM. 2002. Chaotic mixer for microchannels. *Science* 295(5555):647–51
126. Cooney C, Chen C, Emerling M, Nadim A, Sterling J. 2006. Electrowetting droplet microfluidics on a single planar surface. *Microfluid. Nanofluid.* 2(5):435–46
127. Paik P, Pamula VK, Fair RB. 2003. Rapid droplet mixers for digital microfluidic systems. *Lab. Chip* 3(4):253–59
128. Paik P, Pamula VK, Pollack MG, Fair RB. 2003. Electrowetting-based droplet mixers for microfluidic systems. *Lab. Chip* 3:28–33
129. Gao X, Zhou X, Gulari E. 2003. Light directed massively parallel on-chip synthesis of peptide arrays with *t*-Boc chemistry. *Proteomics* 3(11):2135–41
130. Tan Y, Fisher JS, Lee AI, Cristini V, Lee AP. 2004. Design of microfluidic channel geometries for the control of droplet volume, chemical concentration, and sorting. *Lab. Chip* 4(4):292–98
131. Ting TH, Yap YF, Nguyen NT, Wong TN, Chai JC, Yobas L. 2006. Thermally mediated breakup of drops in microchannels. *Appl. Phys. Lett.* 89:234101
132. Link DR, Anna SL, Weitz DA, Stone HA. 2004. Geometrically mediated breakup of drops in microfluidic devices. *Phys. Rev. Lett.* 92(5):054503
133. Cho SK, Zhao Y, Kim CJ. 2007. Concentration and binary separation of micro particles for droplet-based digital microfluidics. *Lab. Chip* 7(4):490–98
134. Chabert M, Viovy J. 2008. Microfluidic high-throughput encapsulation and hydrodynamic self-sorting of single cells. *Proc. Natl. Acad. Sci. USA* 105(9):3191–96
135. Link DR, Grasland-Mongrain E, Duri A, Sarrazin F, Cheng Z, et al. 2006. Electric control of droplets in microfluidic devices. *Angew. Chem. Int. Ed.* 45:2556–60
136. Baroud CN, Delville J, Gallaire F, Wunenburger R. 2007. Thermocapillary valve for droplet production and sorting. *Phys. Rev. E* 75(4):046302
137. Ahn K, Kerbage C, Hunt TP, Westervelt RM, Link DR, Weitz DA. 2006. Dielectrophoretic manipulation of drops for high-speed microfluidic sorting devices. *Appl. Phys. Lett.* 88(2):024104
138. Baret J, Miller OJ, Taly V, Ryckelynck M, El-Harrak A, et al. 2009. Fluorescence-activated droplet sorting (FADS): efficient microfluidic cell sorting based on enzymatic activity. *Lab. Chip* 9(13):1850–58
139. Burns MA, Johnson BN, Brahmasandra SN, Handique K, Webster JR, et al. 1998. An integrated nanoliter DNA analysis device. *Science* 282(5388):484–87
140. Zhang Y, Park S, Yang S, Wang T. 2010. An all-in-one microfluidic device for parallel DNA extraction and gene analysis. *Biomed. Microdevices* 12(6):1043–49
141. Li L, Du W, Ismagilov R. 2010. User-loaded SlipChip for equipment-free multiplexed nanoliter-scale experiments. *J. Am. Chem. Soc.* 132(1):106–11

142. Granieri L, Baret JC, Griffiths AD, Merten CA. 2010. High-throughput screening of enzymes by retroviral display using droplet-based microfluidics. *Chem. Biol.* 17(3):229–35
143. Han Z, Li W, Huang Y, Zheng B. 2009. Measuring rapid enzymatic kinetics by electrochemical method in droplet-based microfluidic devices with pneumatic valves. *Anal. Chem.* 81(14):5840–45
144. Ehrnström R. 2002. Profile: Miniaturization and integration: challenges and breakthroughs in microfluidics. *R. Soc. Chem.* 2:26N–30N
145. Oita I, Halewyck H, Thys B, Rombaut B, Vander Heyden Y, Mangelings D. 2010. Microfluidics in macro-biomolecules analysis: macro inside in a nano world. *Anal. Bioanal. Chem.* 398(1):239–64
146. Manz A, Graber N, Widmer H. 1990. Miniaturized total chemical analysis systems: a novel concept for chemical sensing. *Sens. Actuators B* 1(1–6):244–48
147. Huh D, Mills KL, Zhu X, Burns MA, Thouless MD, Takayama S. 2007. Tuneable elastomeric nanochannels for nanofluidic manipulation. *Nat. Mater.* 6(6):424–28
148. Bocquet L, Charlaix E. 2010. Nanofluidics, from bulk to interfaces. *Chem. Soc. Rev.* 39(3):1073–95
149. Burns MA. 2002. Everyone's a (future) chemist. *Science* 296(5574):1818–19

Annual Review of Chemical and Biomolecular Engineering

Volume 2, 2011

Contents